

8.3.3. Moisture Content And Bulk Density

Variations in the moisture content and bulk density of selected cores from the Central Basin are given in Table 8.2. At LP5, the lowest 70 cm of the core have a consistent water content of around 70%. In the upper 100 cm there is a slight increase in moisture content to 73-81%, with the amount increasing up the core. The water content of sediments from LP10 is similar to that at LP5 (Table 8.1).

In general, there is a greater amount of water in the upper part of the cores collected from the Southern Basin. However, as with those cores collected from the Southern Basin the ostracode-rich and organic sediments tend to have a slightly greater water content than the clays:

The bulk density of the sediment is relatively low for all the sediment types. At LP5 bulk density varies from 0.29 to 0.37 in the bottom part of the core and is even less, between 0.22 and 0.3 in the upper 100 cm of the core.

8.3.4. Carbonate Content

Determination of the carbonate content of the MC was performed by ignition at 1000°C (Saporito, 1975). The results from his analysis are shown in Figure 4.7. In contrast to results obtained by gasometric measurements in this investigation, Saporito (1975) recorded peaks of CaCO_3 associated with the clay units, while ostracode-rich sediments displayed relatively low values. Furthermore, he obtained an inverse relationship between CaCO_3 results and Ca content as determined by atomic absorption, his carbonate curve appears to be spurious and actually reflects moisture loss from the lattice of clay minerals at such high temperatures.

In core LP5, there is a noticeable decrease in the CaCO_3 content from the base to the upper part of the core (Fig. 8.3). Between 170 and 189 cm, the CaCO_3 content is about 4-8%. It increases sharply at 170 cm, exhibiting a peak of 25% at 163 cm, but declines markedly above this level. A second, smaller peak is seen at 110 cm. In the

upper 100 cm of this core, CaCO_3 accounts for less than 5% of the dry weight of the sediment.

CaCO_3 is found only in very small amounts in the sediments from LP10. Between 90 and 190 cm, very little CaCO_3 was measured. A small peak of CaCO_3 is seen between 60 and 80 cm, accounting for 13% of the dry weight of the sediment. In the upper 60 cm, 4-5% CaCO_3 content is found.

With the exception of LP5 and LP6, the cores from the Central Basin all contain very small amounts of CaCO_3 , generally accounting for less than 5% of the dry weight of the sediment. In all instances higher CaCO_3 values were recorded on those sediments rich in ostracodes and/or organic matter.

8.3.5 Loss-on-ignition

The organic content of the MC was assessed by Saporito (1975) using loss-on-ignition at 500°C . High L.O.I levels were found between 256 and 336 cm, these ranging from 20 to 40 % with a large peak seen between 260 and 270 cm. A marked decrease to approximately 10 % organic matter occurs at 256 cm which coincides with the boundary between the gyttja and ^{clay} . There is a gradual increase in L.O.I to approximately 30% at 167 cm. L.O.I. levels of 10-12% are found between 117 and 167 cm and are associated with the change to the clay material. With the exception of a large peak (28 %) at approximately 97 cm coincident with the ostracode rich layer at this point, L.O.I. remains at approximately 10-11% up core.

LP5 is characterised by L.O.I. values of 15 to 25%. At the base of the core, the sediments contain approximately 25% organic matter. The measured values decrease to approximately 15% between 110 and 130 cm, but increase again to 25% at 100 cm. In the upper 100 cm of the core, there is approximately 15% organic matter within the sediments.

Slightly lower L.O.I. values are recorded for LP10. The sediment at the base of this core contains approximately 15 % organic matter. This increases up the core with a

peak at 168 cm, coinciding with the ostracode-rich sediments. Above this level, the measured values generally vary between 10 and 15%, although a second smaller peak is observed between 60 and 80 cm. In the upper part of the core, organic matter accounts for approximately 15% of the dry weight of the sediment.

The L.O.I. curves from other cores in the Central Basin are similar to those described for LP10 and the MC: the layers rich in ostracodes generally contain a greater amount of organic matter than the clay units (Fig. 8.3). LP5 differs in that its L.O.I. is very high. This probably reflect the fact that this core was taken close to the lake shore in very shallow water; and thus the content of plant detritus in the sediments may always have been very high.

8.3.5 Magnetic Susceptibility (X)

X was measured for the entire MC. Only the results from the Holocene part of the core will be given here. At 4.23 m (the Pleistocene/Holocene boundary) a small peak in X is noted. X levels between 423 and 350 cm are low, being approximately $10\text{--}12 \text{ E-}06 \text{ kg m}^{-3}$. An increase in X to $13\text{--}14 \text{ E-}06 \text{ kg m}^{-3}$ is noted between 350 and 320 cm with a further peak of similar magnitude between 260 to 230 cm. An abrupt increase in X to approximately $500 \text{ E-}06 \text{ kg m}^{-3}$ occurs at 220 cm remaining at this level until 180 cm with the sediments between 150 and 120 cm having a X of about $20 \text{ E-}06 \text{ kg m}^{-3}$. In the upper part of the core, two peaks in X are seen (Fig.4.7) The lower forms a sharp peak with X values of nearly $400 \text{ E-}06 \text{ kg m}^{-3}$ followed by an equally rapid trough in X . X values in the upper 97 cm of the core are in the order of $400\text{--}500 \text{ E-}06 \text{ kg m}^{-3}$.

With the exception of a small part of the core between 130 and 150 cm the sediments at LP5 are characterised by high X values. The peaks in the lowest 30 cm of the core are of a much smaller magnitude than those found above 130 cm. A sharp increase in X is noted at 130 cm, but it decreases again between 100 and 110 cm prior to returning to high levels and remaining as such up the core.

The X curve for LP10 displays much more distinct peaks. A sharp peak at the

base of the core, with X values as high as $550 \text{ E-06 kg m}^{-3}$ is followed by relatively low X levels between 170 and 180 cm. X increases markedly at 160 cm, to levels of around $600 \text{ E-06 kg m}^{-3}$, remaining high until approximately 90 cm. Between 70 and 90 cm X levels hover around $50\text{-}60 \text{ E-06 kg m}^{-3}$. A gradual increase in X occurs in the upper 60 cm of the core.

It is evident from the X curves of the other six cores taken in the Central Basin that there are differences in the pattern of variations between sites in this part of the lake; LP5 and LP6 displaying quite a different record to the other cores. LP6, in particular, exhibits a considerable number of peaks, many in the bottom part of the core being of a relatively small magnitude. It is possible that the position of this core near the shore of the lake means that a much greater period of sediment accumulation is covered, and that the three main peaks in the upper part of the core correspond to those seen at other sites in this part of the basin. In the case of LP5, although there is a decrease in X at approximately 100 cm it is not as marked as that seen at other cores in this area. This suggests that sediment input in this part of the basin has been continuous over the last 3,000 years.

8.3.7. Grain Size

Grain size was measured on three cores from the Central Basin, LP5, LP7 and LP10. At the base of LP5 the mean grain size is approximately $15 \mu\text{m}$, increasing to over $20 \mu\text{m}$ at 140 cm (Fig. 8.3). A decrease in mean grain size, to $8 \mu\text{m}$, occurs between 130 and 140, with a more gradual decrease occurring above 130 cm. In the upper 70 cm is around $5 \mu\text{m}$.

In contrast the mean grain size for LP7 remain relatively consistent throughout the core with the exception of 160-170 cm and 60-70 cm where the sediments are slightly coarser, having a mean grain size of approximately $15 \mu\text{m}$.

Variations in the mean grain size of the sediments from LP10 are shown in Figure 8.3. Like LP7, sediments are very fine, having a mean grain size of about $10 \mu\text{m}$.

The coarsest sediments are found at the base of the core and between 60 and 80 cm where they have a maximum mean grain size of $14\mu\text{m}$. In the upper 60 cm of the core the mean grain size is between 3 and $7\mu\text{m}$.

The relationship between mean grain size and stratigraphy is apparent at all the sites investigated in the Central Basin and confirmed by analyses. In general, the coarsest sediments tend to be organic or to contain a high amount of ostracodes. Sediments that have been washed into the basin from the surrounding slopes tend to be much finer, ranging between 3 and $8\mu\text{m}$. A similar relationship was also noted at LP11.

8.3.8 Summary and Interpretation of the Central Basin Sediments

Unlike the other cores, the MC provides a complete record of the Holocene sediment accumulation in the Central Basin. X levels at the base of this core indicate a short-lived period of sediment influx into the lake approximately 9,000 years B.P. Between 9,000 and approximately 5,000 years ago there appears to have been little clastic input into the lake. A small peak in X between 330 and 310 cm dates to approximately 5,000 years B.P. The pollen assemblage from this core segment indicates a decrease in *Alnus* which has been interpreted by Watts and Bradbury (1982) as indicating either a slight shift to drier conditions, or the cutting down of riparian alder by early settlers in the basin. A small peak in X dating to approximately 3,500 years ago coincides with the first appearance of maize in the pollen record, indicating the presence of sedentary agriculture within the basin; this may have triggered erosion within the basin. The date of this erosional event is almost identical to the date on the oldest episode recorded at LP11 in the Southern Basin. Disturbance within the basin continued for approximately 200-400 years, after which time there appears to have been little sediment entering the lake from the catchment. The sediment which has accumulated above this disturbance is high in organic matter and exhibits a low X .

A marked change in stratigraphy occurs at 180 cm with a shift from sediments

rich in organic matter and having a low X to a fine clayey sediment containing little organic matter and having very high X levels. This evidence clearly indicates a marked shift in sediment origin from one dominated by sediments produced by the lake itself to a situation where sediments are entering the lake from the catchment. A date of 2,890 ± 80 on sediment immediately below this change in stratigraphy is available (Watts and Bradbury, 1982). Assuming a constant rate of sediment accumulation this would place the onset of erosion within the basin at approximately 2,500 years ago. A similar date is recorded on the beginning of sediment accumulation at both LP5 and LP11 in the Southern Basin, and clearly indicates widespread disturbance within the basin at this time.

The results of this investigation indicate that over the last 2,500 years sediment accumulation in this part of the basin has been dominated by clastic input from the catchment. Between 120 and 97 cm, however, the sediment record from the MC indicates a reduction in sediment from the catchment accumulating at this site.

At no point in the past 2,900 years has there been a cessation in sediment entering the lake at LP5, although there is a decrease in X dating to approximately 1,500. This is associated with a layer of ostracode-rich sediments and it is possible that their presence has 'diluted' the mineral magnetic signal and that there has been continuous disturbance in this part of the basin over the last 3,000 years.

8.4 THE NORTHERN BASIN

Six cores, LP14, LP16, LP17, LP18, LP19, and LP20, which vary in length from 1.24 m to 2.8 m, were collected from the northern part of the lake (Figs. 8.1 and 8.4). Although a similar stratigraphy was noted at all sites the large quantity of ostracodes present in LP19 made this core the most suitable for the extraction of material for dating purposes. In view of this, LP19 has been taken to represent the Northern Basin, and was analysed in greater detail than the other cores.

8.4.1. Stratigraphy

A 2.4 m long core was collected at LP19, approximately 1 km from the lake shore north of the town of Tzintzuntzan. The lake depth at this point was 5 m. The basal unit comprises 25 cm (215-240 cm) of ostracode-rich sediment. This material has a relatively silty texture and is notably rich in organic and root remains. The concentration of ostracode shells increases in the upper part of the unit. These sediments are overlain by a 59 cm unit (156-215 cm) of smooth, very dark greyish brown (10YR 3/2) clay. A second ostracode-rich layer is found between 145 and 156 cm. Abundant vegetation remains are associated with this layer. The upper most unit consists of 145 cm of smooth unstructured clay, similar in appearance and colour to the underlying clay unit.

There is a remarkable similarity between the stratigraphy at all six sites in this part of the basin, although there are considerable variations in the thickness of individual units. LP14, for example, is only 1.24 m in length, but all four units described in LP19 are present. In general, the lower clay unit is thickest in the north-eastern part of the basin while the upper unit is most extensive in the western part (Fig. 8.4).

8.4.2 Radiocarbon Dates And Sediment Accumulation Rates

Dates were obtained from the two ostracode-rich sediment layers in LP19. Ostracodes extracted from 223 cm, at the boundary between the lower ostracode-rich layer and the lower clay, yielded a date of $2,530 \pm 60$ years (OaX-2823). Those extracted from 149-150 cm yielded a date of 880 ± 60 years (OaX-2823). Using these dates it is possible to estimate the sediment-accumulation rate at this site. In the lower part of the core between 150 and 223 cm, sediment accumulated at a rate of 4.4 cm/100 years. A marked increase in sedimentation to 16 cm/100 years has occurred in the last 900 years.

8.4.3 Moisture Content And Bulk Density

The moisture content of LP19 varies between 69 and 81%. At the base of the core, the sediments contain up to 75% moisture with a slight decrease in the lower of

the two clay layers. A marked increase in moisture content is noted in the upper clay, which contains 73-81% moisture increasing up the core. The results from LP19 are similar to those measured on other cores in the Northern Basin, with ostracode layers generally having a greater moisture content than the clay units.

8.5.4 Carbonate Content

In general, the carbonate content of the sediment from LP19 is low (Fig. 8.3). At the base of this core values of less than 2 % are found. A sharp peak in CaCO_3 to 22% is observed at 215 cm but this drops to low levels by 210 cm. A second large peak (28% dry weight) is seen at 145 cm. In the upper part of the core, carbonate content remains low, and stable, being approximately 2 to 3%. As expected, peaks in carbonate content correspond to layers rich in ostracodes. Although this pattern is observed at all the sites in the Northern Basin, the size and magnitude of peaks does vary between sites.

8.4.5. Loss-on-ignition

Only a small amount of organic matter is contained within the sediments at LP19. At the base of the core L.O.I. ranges from 15 to 20%, it gradually decreases upwards but is somewhat lower in the clay units than the ostracode-rich sediments. In the upper clay unit there is approximately 10 to 12% organic matter by dry weight. The amount of organic material within the sediments at other cores in this region exhibits a similar pattern (Fig. 8.3); the clay units having approximately 10 to 12% organic matter while the ostracode-rich layers generally correspond with peaks in L.O.I. as high as 25%.

8.4.6 Magnetic susceptibility (X)

LP19 is characterised by very high levels of X (Fig. 8.4). At the base of the core X is low, although a small peak is seen between 215 and 223 cm. An extremely large peak in X with levels as high as 600 to $700 \text{ E-06 kg m}^{-3}$ is noted between x and x cm and corresponds to the lower of the two clay units. X decreases markedly at 150 cm and

remains low for 10 cm before rising rapidly to even higher levels (800 to 900 E-06 kg m⁻³).

The variations in X with depth for the other cores from the northern basin are remarkably similar to those seen at LP19 (Fig. 8.3), although in no instance does X attain such high values. The size of individual peaks does vary from site to site, for example at LP16 the upper peak is much larger than the lower one, while at LP17 the reverse is seen. In all cases, however, there is a general up profile increase in X in the case of the upper most peak (Fig. 8.3).

8.4.7 Grain Size

The sediments in core LP19 are extremely fine and consist predominantly of clay-sized material (Fig. 8.4). Between 240 and 200 cm, there is a gradual decrease in mean grain size from 14 to 5 μm remaining at the latter level until 160 cm. At this level there is a marked increase in mean grain size to 17 μm at 150 cm. The grain size then decreases again immediately after this before exhibiting a second small peak at 120 cm. The sediment above this level is extremely fine and in general has a mean grain size of less than 3 μm .

8.4.9 Summary and Interpretation of the Northern Basin Sediments

The sedimentary record at LP19 covers at least the last 2,600 years. Over this interval the sediment composition at this site has been dominated by the input of detrital material from the catchment. At the base of the core there is a unit of silty sediment with relatively high organic and carbonate content. At 215 cm we observe a change to sediments dominated by clay which are low in CaCO_3 , and organic matter, but display high X levels. The physical properties of this core indicate that this unit is dominated by clastic sediment and implies disturbance in the lake catchment at the time of accumulation. This period of disturbance is bracketed by two dates, 2,530 years B.P. and 880 years B.P.

A thin ostracode layer accumulated at LP19 at approximately 880 years B.P. after which time sediments accumulating at this site are dominated by sediment influx from the basin.

The stratigraphy and physical properties of other cores collected from the northern part of Lake Pátzcuaro all exhibit very similar features. In all cases at least two episodes of erosion can be inferred, although the amount of accumulation varies at different sites. In general, however, sediment accumulation has been greatest at those sites situated in the north east part of the lake.

8.5 SUMMARY AND INTERPRETATION OF THE PHYSICAL PROPERTIES OF THE LAKE SEDIMENT RECORD

Twenty-one cores from Lake Pátzcuaro have been analysed and provide the basis for determining episodes of disturbance within the catchment. Of the different stratigraphical units identified, three were recognized at all core sites; a lower clay unit, an ostracode-rich layer and an upper clay unit. The clays are associated with the two most recent erosional events within the catchment. Even though it has been possible to identify these three units, differences in the basic physical properties are noted across the basin.

In general, cores from the Southern Basin have a higher moisture content than those collected in the north. The difference is particularly noticeable in the lower of the two clay units with cores in the south containing about 10% more water. The difference in moisture content could be due to a number of factors. The most obvious of these is that there has been a greater thickness of sediment accumulation in the Northern Basin causing greater sediment compaction this may have been exacerbated by the greater depth of water that is also found in the northern part of the lake.

There are marked variations in the CaCO_3 content of the sediments in different parts of the lake, those cores from the Southern Basin having a much greater CaCO_3 content than cores from other parts of the lake. The difference in CaCO_3 content across

the lake is much greater for the lower clay unit than for other stratigraphical units. It is possible that variations in the CaCO_3 content are a reflection of productivity within the lake. This variation in the CaCO_3 content of sediments from different parts of the lake may be a reflection of the depth of the lake. The shallow waters in the Southern Basin allows a greater build up of aquatic vegetation. To enable photosynthesis these plants need to extract dissolved inorganic carbon from the lake waters; as Lake Pátzcuaro has low levels of dissolved CO_2 it is necessary for plants to directly^{ly} assimilate bicarbonate. The net effect of this process is to cause a shift in carbonate equilibrium, resulting in the precipitation of CaCO_3 (Street-Perrott pers. comm., 1991).

Similarly, variations in L.O.I. values across the lake are observed. As with CaCO_3 content, L.O.I. is generally greater in cores from the Southern Basin (Table 8.2). Particularly high L.O.I. levels are recorded for those cores that were collected close to the lake shore. The most important feature of this data set is the marked increase in L.O.I. associated with the ostracode-rich layer, implying greater aquatic vegetation within the lake. It was evident from the stratigraphy that this unit and other ostracode-rich layers contained large quantities of root and vegetation remains. It is possible that during accumulation of these layers the level of the lake was relatively low; this would increase the amount of light that could penetrate to the lake bed, allowing aquatic vegetation to establish. As discussed above, as the lake is undersaturated in respect to CO_2 plants extract calcium bicarbonate resulting in the precipitation of CaCO_3 and providing suitable conditions for ostracodes to flourish.

Another factor that must be considered, however, is the input of clastic material into the lake. It is noted that there is a marked decrease in L.O.I. associated with the clay layers, Input of clays will have increased turbidity, reduced light penetration and thereby inhibiting plant photosynthesis. If light penetration were reduced aquatic vegetation would have less chance of survival in deeper waters and could result in a dramatic change in the chemical status of the lake.

Peaks in X are associated with clay deposits, Δ Sediments that are ostracode-rich

or display high L.O.I. values have low X values. Peaks in X are noted in all cores and provide a method that allows basin wide correlations to be made. X values on cores from the Northern Basin are generally greater than those measured on cores from the Southern Basin indicating a greater quantity of magnetic minerals and thus clastic material in the northern portion of the lake.

Variations in the mean grain size of the lake sediments were noted both in and between core sites. In general, the coarsest sediments are associated with the organic gyttja and ostracode-rich layers. A marked decrease in mean grain size is associated with the clay layers. There is an overall decrease in the mean grain size for the different units from south to north in the lake. This is particularly marked in the upper clay unit with sediments at LP19 being particularly fine compared to those at LP11. As discussed in Chapter 2, Chacón Torres (1989) noted that the water currents of Lake Pátzcuaro move from the south west to the north east along the axis of the lake. It is possible that there is a net transfer of sediment, in particular clays, from the southern to the northern basin. This would add to the amount of material that accumulated in this part of the lake. At the present time there appears to be net transfer of sediment to the northern part of the lake and Chacón Torres (1989) reported much higher levels of suspended sediment in the lake (see Figure 2.).

8.6 CONCLUSIONS

Based on the different analyses of the physical properties it is evident that while the shortest cores were collected from the Southern Basin they provide the longest record of sediment accumulation in the lake. The basic stratigraphy of the lake can be divided into three main types; organic gyttja, ostracode-rich silt and clays, from the basis of stratigraphical and X variations seven main zones can be identified.

8.6.1 Zone 1 (approximately 5,000-4,200 years B.P.)

Sediments associated with this Zone are only found at the MC. Based on X it

would be possible to delimit further zones, however, only those sediments in the upper 3.36 m of the core are of relevance to this study as they represent the last 5,000-6,000 years of sedimentation. A small peak in X at the top of Zone I is believed to indicate increased sediment input into the lake in response to a slight shift to drier climate.

8.6.2 Zone II (approximately 4,200-3,600 years B.P.)

Sediments related to this zone are only present at cores in the Southern basin and at the MC. These sediments are characterised by low X , and high CaCO_3 and L.O.I. values and indicate a period of stability within the catchment and little input of clastic material into the lake. The high level of CaCO_3 in these sediments may indicate lower lake levels associated with a period of relative aridity.

8.6.3 Zone III (approximately 3,600 to 3,200 years B.P.)

Slightly higher X values and decrease in CaCO_3 and L.O.I. values characterises Zone III, which also coincides with the first appearance of maize in the pollen record. This period of increased clastic influx is believed to be a result of human disturbance within the basin.

8.6.4 Zone IV (approximately 3,200 to 2,500 years B.P.)

A period of stability within the drainage basin can be inferred from the physical properties during this period. Sediments from this zone are characterized by Low X and relatively high L.O.I. and CaCO_3 content, they are also rich in ostracodes and root remains. The large peak in CaCO_3 observed at a number of sites is interpreted as indicating lower lake levels during accumulation of these sediments.

8.6.5 Zone V (2,500 to 1,200 years B.P.)

A dramatic increase in X and a drop in L.O.I. and CaCO_3 content are the main features of Zone V. These changes are associated with the influx of clastic material into

the lake and sediments relating to this zone are recognized at all the cores collected. It is clear that sediment accumulation during this phase of disturbance was greatest in the northern and central portion of the lake with only a small quantity of clastic sediment influx into the southern basin.

8.6.6 Zone VI (1,200-850 years B.P.)

The physical properties of the lake sediments during this period all indicate a period of decreased sediment input into the lake. In addition, lower lake levels are inferred from the increase in CaCO_3 and L.O.I. levels. Increases in L.O.I. are particularly marked at those cores that were collected in shallower waters. The presence of tule reeds at LP3 suggest that the lake could have been as much as 3-4 m lower than the 1988 level of 2,036.5 m which would have resulted in desiccation of much of the southern arm of the lake.

8.6.7 Zone VII (850-0 years B.P.)

The most recent phase of disturbance within the catchment began approximately 850 years ago and has continued until the present. As with **Zone V**, there has been a greater accumulation of sediment in the northern part of the lake. This probably reflects the greater degree of environmental degradation in this part of the basin, although it is likely that there has been a net transfer of fine silts and clays from the southern to the northern basin by lake water currents.

CHAPTER NINE: SEDIMENT CHEMISTRY RECORD OF LAKE PATZCUARO

9.1 INTRODUCTION

The sediment chemistry of four cores from Lake Pátzcuaro; LP11, MC, LP10 and LP19 was analysed. The results and discussion of the analysis will be given in this chapter. Samples from the four cores were taken every 5 or 10 cm and prepared using the technique outlined by Engstrom and Wright (1984). Analysis was by A.A.S. and A.A. as described in Chapter 5. In the case of the MC only the upper 3.36 m of the core was analysed as this represents the last 5,000-6,000 years of sediment accumulation at this site, and more than covers the time period under consideration in this thesis.

Once the analysis was complete down core plots for each element were produced using the Micrografx CHARISMA plotting package (1990). To enable the sediment chemistry to be described each core was divided into a number of zones. Zonation was on the basis of stratigraphical and X variations and the designation of these zones is the same as that outlined in Chapter Eight.

Chemical data may be represented either in units of concentration or as rates of accumulation. Although accumulation rates eliminate the problem of covariance between different components it is necessary to have excellent dating control otherwise calculations of influx will have large errors. Even though there is good dating control on the cores collected in this study it is still insufficient to allow reliable accumulation rates to be calculated. The following descriptions will only describe the relative trends in the core sediment chemistry. Exact concentration figures in mg/g for each element are provided by the graphs and are given in Appendix C. The results and discussion for each core will be given separately, beginning in the Southern Basin and progressing northwards to the Northern Basin.

9.2 LAKE PATZCUARO 11

9.2.1 Sediment Chemistry

Six main zones can be distinguished at LP11 (Zone II to Zone VII) and will be used to describe the salient features of the sediment chemistry record (Fig. 9.1). **Zone II**, 189-165 cm, is characterised by relatively low values of Fe(a), Al(a), and Ti(a). Although a small peak in Fe(c), Al(c), Ti(c), Mg(c), Mn(c), Si(c), and K(c) is observed, these elements are only found in similar quantities to those extracted in the 'a' fraction. While Mg(a), Mn(a), Ca(a), Sr(a), Si(a), are low at the base of this zone they increase in the upper section, peaking at the boundary of Zones II and III. A decrease in K(a) and P(a) occurs upwards through Zone II.

Zone III, 168-148 cm, is characterised by peaks in Al(a), Ti(a), Cu(a), K(a), Zn(a) and Si(b). Fe(a) also peaks in this zone but decreases sharply at 160 cm (Fig. 9.1). Other elements that peak in Zone III are Fe(c), Al(c), Ti(c), Mg(c), K(c) and Si(c). Levels of Mg(a), Mn(a), Ca(a) and Sr(a) are low. The most noticeable feature of **Zone IV**, 148-122 cm, is a large peak in Sr(a), and Ca(a) at 130 cm, although both elements display a marked decline in the upper part of Zone IV. Mg(a) and Mn(a), exhibit a noticeable peak at the boundary between Zone III and Zone IV before decreasing slightly at 145 cm and displaying a second small peak at 130 cm. Those elements extracted in the 'c' fraction exhibit a similar trend to that of the latter two elements. Si(b), after peaking in Zone III, shows a gradual decline in Zone IV.

Fe(a), Zn(a), Ti(a), Cu(a), Mn(a), K(a), Si(a) as well as Fe(c), Al(c), Ti(c), Mg(c), K(c) and Si(c), all exhibit a large peak at the base of **Zone V**, 122 to 78 cm, but decrease in level towards the top of this zone. Mg(a) which drops sharply at the base of this zone increases markedly between 80 and 90 cm. This zone is characterised by low values of Ca(a) and Sr(a). Apart from a small peak at 105 cm P(a) remains fairly stable throughout Zone V. The peak in P(a) coincides with a small, but sharp decrease in

K(a), Si(a), Zn(a), Al(a), and small peaks in Ca(a) and Sr(a). Si(b), which exhibited a marked decrease at the boundary between Zones IV and V, shows a gradual increase up the profile to the boundary of Zones V and VI; a similar curve is displayed by Mg(a).

A very large peak in Si(b) is the main feature of Zone VI, 68 to 78 cm. This is paralleled by a sharp decrease in many other elements measured (Fig. 9.1) except for K(c) and Si(c).

The upper 68 cm of the core, Zone VII, are characterised by relatively high levels of Fe(a), Mn(a), Al(a), Zn(a), Ti(a), Cu(a), K(a), and Si(a) throughout. In the case of Fe(c), Al(c), Ti(c), Mg(c), K(c) and Si(c) these are only found in relatively high levels in the upper 40 cm of this zone, generally forming two distinct peaks (Fig. 9.1). Sr(a) and Ca(a) are present in very small amounts in Zone VII, although a very slight increase is noted in both elements in the uppermost part of the core (Fig. 9.1).

9.2.2 Correlation

The correlation matrix constructed from the sediment chemistry data from LP11 (Table 9.1) clearly indicates strong positive correlations between Fe(a), Al(a), Zn(a), Ti(a), K(a) and Si(a). A particularly strong relationship is noted between K(a) and Fe(a): $r=0.82$, K(a) and Al(a): $r=0.83$, K(a) and Zn(a): $r=0.89$ and K(a) and Ti(a): $r=0.88$. Similarly Ti(a) correlates strongly with Fe(a) ($r=0.83$), Al(a) ($r=0.85$), Zn(a) ($r=0.82$). A very strong correlation between Si(a) and Al(a) ($r=0.83$) is also noted. All the above elements display a negative relationship with Sr(a), Ca(a) and Mg(a) (Table 9.1).

The most positive relationship in the entire data set is observed between Sr(a) and Ca(a) $r=0.96$. The only other element with which Sr(a) and Ca(a) show a positive correlation is Mg(a), with values $r=0.54$ and $r=0.58$ respectively.

Fe(c), Al(c), Ti(c), Mg(c) and K(c) all exhibit a relatively strong positive correlation with one another (Table 9.1), but have little association with other elements. Si(b) is interesting in that it exhibits little relationship with other elements in the data set.

Table 9.1 Correlation matrix from sediment chemistry data set from LP11

	Fe(a)	Al(a)	Zn(a)	Ti(a)	Cu(a)	Mg(a)	Mn(a)	Ca(a)
0.793								
0.854	0.778							
0.834	0.849	0.822						
0.277	0.203	0.203	0.207					
-0.457	-0.354	-0.475	-0.444	-0.221				
0.555	0.376	0.358	0.398	0.177	0.003			
-0.517	-0.587	-0.706	-0.617	-0.165	0.578			
-0.415	-0.524	-0.611	-0.520	-0.054	0.541	0.139		0.959
0.815	0.826	0.885	0.880	0.327	-0.407	0.226		-0.728
0.754	0.830	0.780	0.752	0.199	-0.259	0.316		-0.554
-0.507	-0.515	-0.480	-0.551	-0.222	0.100	-0.377		0.339
-0.332	-0.082	-0.223	-0.149	-0.056	0.319	-0.337		0.007
0.166	0.105	0.164	0.198	-0.088	-0.169	0.326		-0.213
0.426	0.300	0.313	0.436	0.015	-0.197	0.461		-0.266
0.485	0.342	0.440	0.343	0.018	-0.310	0.468		-0.417
-0.382	-0.397	-0.400	-0.424	-0.288	0.174	-0.144		0.187
0.021	-0.008	0.014	-0.117	-0.148	-0.198	0.010		-0.178
-0.056	-0.114	-0.006	-0.114	-0.219	-0.042	-0.144		-0.183
-0.010	-0.103	-0.148	-0.171	-0.152	-0.086	0.176		0.037
0.060	0.079	0.004	0.068	-0.054	-0.113	0.012		-0.013
Sr(a)	K(a)	Si(a)	P(a)	Si(b)	Fe(c)	Al(c)	Ti(c)	
-0.593								
-0.503	0.759							
0.217	-0.588	-0.469						
-0.010	-0.058	-0.124	-0.163					
-0.228	0.129	0.202	-0.249	0.019				
-0.209	0.332	0.346	-0.454	0.056	0.787			
-0.409	0.363	0.432	-0.443	-0.143	0.770	0.702		
0.065	-0.432	-0.342	0.159	0.018	0.346	0.029	0.283	
-0.278	-0.065	0.165	-0.091	-0.029	0.578	0.295	0.606	
-0.224	-0.019	-0.102	-0.081	0.155	0.446	0.312	0.461	
0.004	-0.109	-0.004	0.024	-0.272	0.214	0.168	0.267	
-0.048	-0.016	-0.066	-0.022	-0.119	0.092	0.068	0.061	
Mg(c)	K(c)	Si(c)	Mn(c)					
0.696								
0.607	0.637							
0.191	0.222	0.146						
0.292	0.215	0.164	0.101					

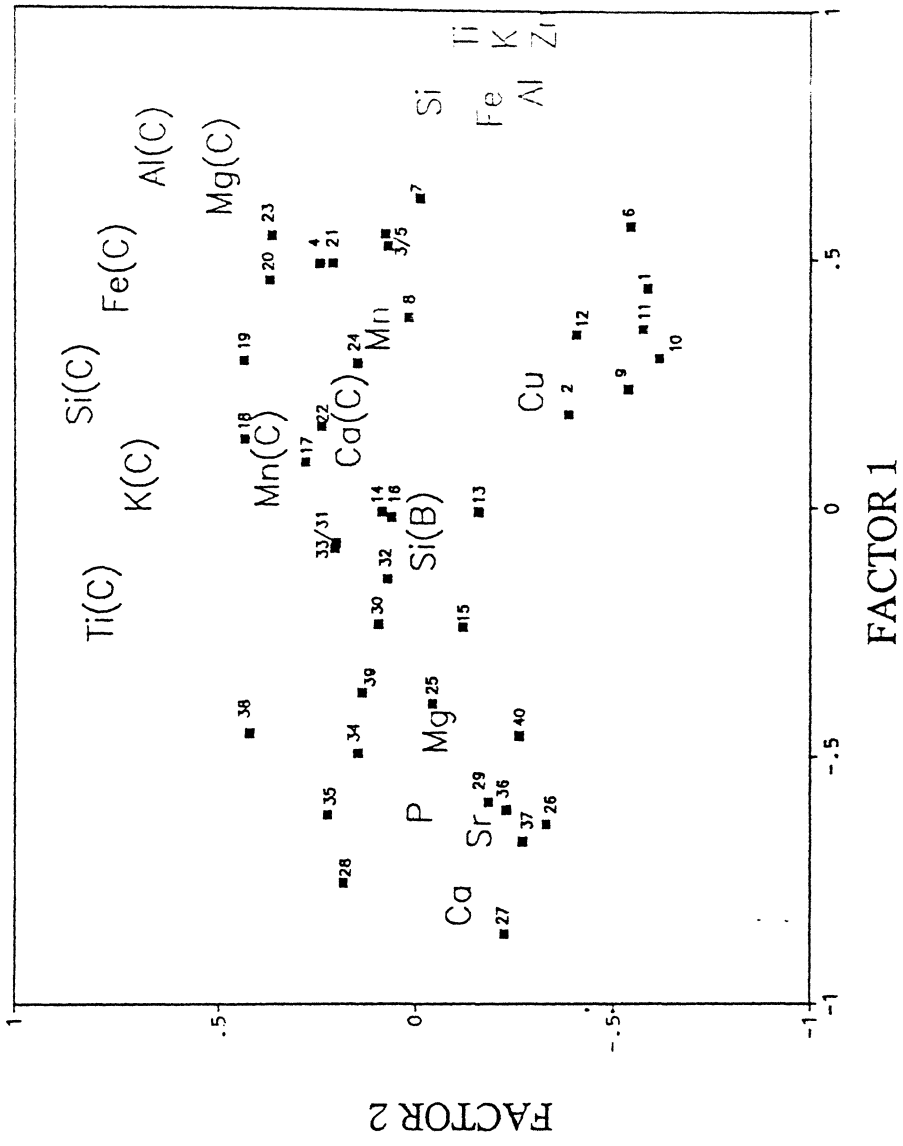
9.2.3 Factor Analysis

The results of the factor analysis on the geochemical data set from LP11 are shown in figures 9.2 and 9.3. Factors 1, 2 and 3 account for 36.32%, 17.76% and 10.04% of the variability within the data set respectively. Figure 9.2 shows the distribution of variables and samples in 'factor space' in relation to Factors 1 and 2. Si(a), Fe(a), Al(a), Zn(a), K(a) and Ti(a) all cluster together and load very highly on Factor 1, while loading slightly negatively on Factor 2. Other variables that load positively, but less strongly on Factor 1 are Mn(a), Cu(a) Mg(c), Al(c) and Fe(c). The latter three elements also load positively on Factor 2 together with Si(c), K(c) and Ti(c). Clustered together exhibiting a strong negative loading on Factor 1 are Ca(a), Sr(a), Mg(a) and P(a).

Several sample clusters can be distinguished on the plot of Factor 1 versus Factor 2. Two sample clusters plot positively on Factor 1, the largest of which also loads positively on Factor 2. This group of samples plots between two variable groups, one consisting of Ti(c), K(c), Si(c), Fe(c), Al(c), Mg(c), Mn(c) and Ca(c) and a second comprising Si(a), Fe(a), Ti(a), K(a) Al(a), Zn(a) and Mn(a). This indicates that the sediment chemistry of the samples which plot between these two variable samples are made up of material extracted in both the 'a' and 'c' fractions and suggests that they are a product of both weathered and unweathered material.

A second group of samples which loads positively on Factor 1, is strongly negative on Factor 2 and plots closely with elements extracted in the 'a' fraction and has little relationship with variables from the 'c' fraction. This relationship with the different variable groupings indicates that these samples are dominated by weathered material entering the lake from the catchment.

All the samples that load positively on Factor 1 come from the middle and upper clay layer at LP11 (Fig. 9.3). Samples from the middle unit all load positively on Factors 1 and 2 in a similar position to those variables extracted in the 'c' fraction and suggested that these sediments are dominated by unweathered material. A number of samples



Sample numbers

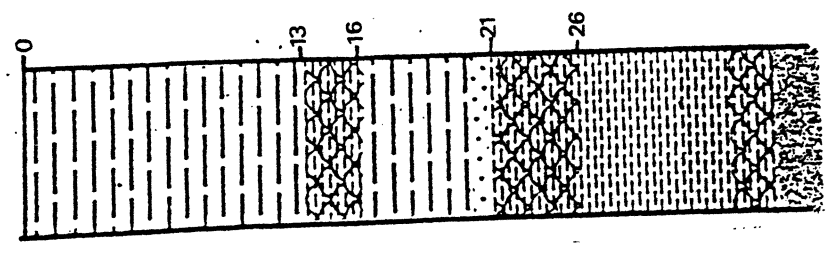


Figure 9.2 Distribution of samples and variables on Factors 1 versus Factor 2 for LP11. Samples locations shown against core stratigraphy.

Sample numbers

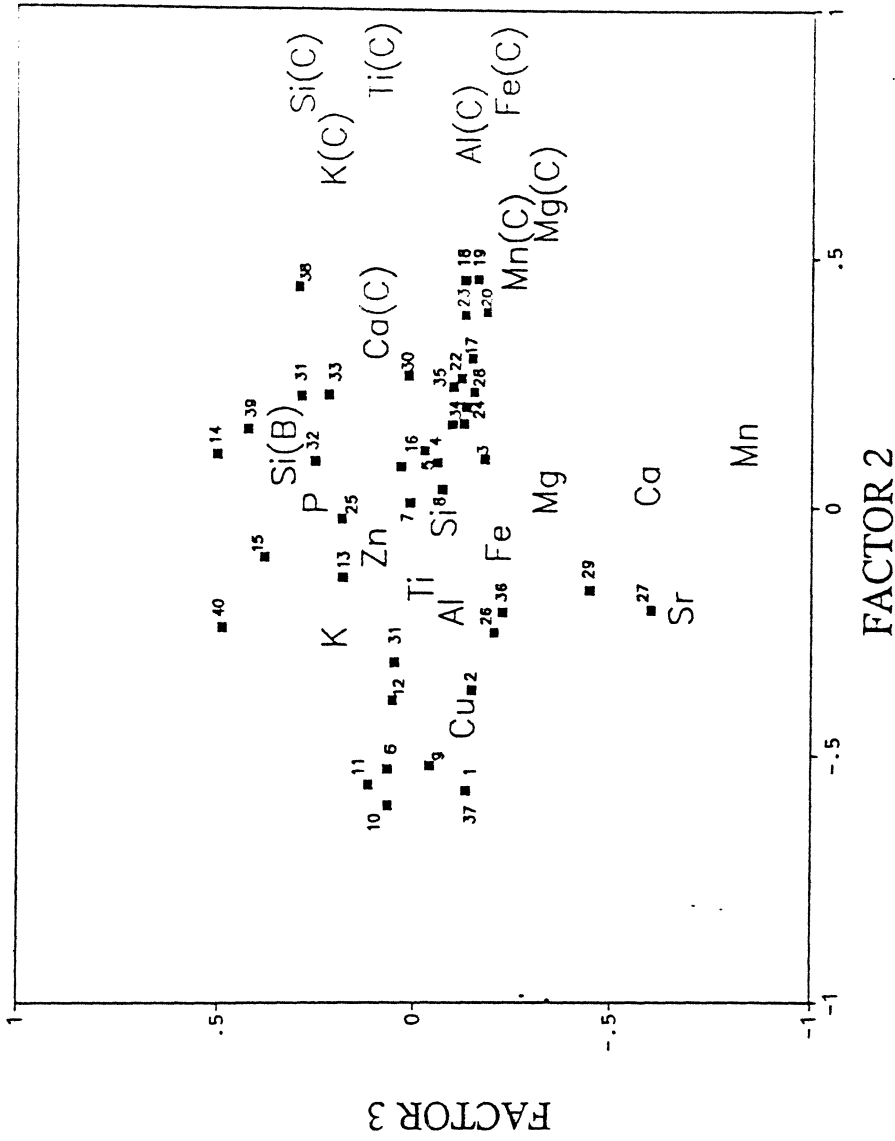
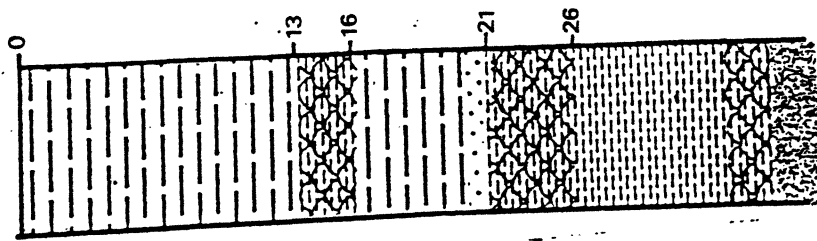


Figure 9.3 Distribution of samples and variables on Factors 2 versus Factor 3 for LP11. Samples locations shown against core stratigraphy.

from the upper clay unit are also located in this cluster, although they tend to be located between the two variables groupings, indicating that the sediment make-up is of both weathered and unweathered material. Those samples that load positively on Factor 1, but negatively on Factor 2 are all from the uppermost unit and are closely associated with weathered material entering the basin from the catchment.

A large number of samples load negatively on Factor 1. Apart from a small group of samples that load slightly negatively on Factor 2, most form a general scattering of samples that load slightly positively on Factor 2. Most of the samples in these two clusters are from the base of LP11 where the sediment is made up of gyttja and ostracode rich sediments. Although some of these samples load positively on Factor 2 and show some relation to those variables extracted in the 'c' fraction, most indicate that only a minimal amount of sediment from the catchment was been deposited in the lake during their accumulation.

A number of variable groupings can be distinguished on the plot of Factor 2 versus Factor 3 (Fig. 9.3). As discussed, the clearest controls on Factor 2 are those elements extracted in the 'c' fraction with Fe(c), Al(c), Ti(c) and Si(c) showing the most positive loadings. Sr(a), Ca(a) and Mn(a) have little influence on Factor 2, but exhibit a strong negative loading on Factor 3. The remaining variables all cluster together in the central part of the plot indicating that they have little influence over either of these Factors.

There is a strong central clustering of samples on the plot of Factor 2 versus Factor 3, although a number of samples do plot away from the main group. A small cluster of samples which load slightly positively on Factor three, but do not influence Factor 2 are also noted. In addition two samples, 27 and 29, exhibit a strong negative loading on Factor 3.

The majority of samples on the plot of Factor 2 versus Factor 3 are located between the two groups of variables that indicate weathered and unweathered catchment material. Another assemblage which loads negatively on Factor 2, but does

not influence Factor 3 appears to be closely associated with weathered catchment material. A large number of samples cluster around Si(b) and load positively on Factor 3, while two samples load negatively on Factor 3 and are closely associated with Mg(a), Ca(a), and Sr(a).

Down-core variations in Factor loadings for the first three Factors are shown in Figure 9.4. Factor 1 which explains 36.32% of the variations is not the most important Factor in the lower part of the core. It is only at approximately 125 cm that those variables that load on Factor 1 dominate the core sediment chemistry. It is interesting to note that this curve closely reflects the curve of magnetic susceptibility at this site (see Figure 9.1).

In comparison Factor 2 which is explained by the input of unweathered material into the lake is much more important in the lower part of the core than the upper section, although between 80 and 120 cm the two Factors appear to be equally important. Factor 3 which accounts for 10.04 % of the variations is again most important in the lower 70 cm of the core and is mainly described by Si(b) and P(a). This may possibly relate to lake productivity.

9.2.4. Summary Of LP11

The following summary of the lake sediment record from LP11 will also draw on evidence presented in Chapter Eight relating to the physical properties of the core. It is possible to divide the sediment chemistry record of LP11 into two broad divisions. The lower of these, 189-120 cm is dominated by those elements that indicate sediments accumulating in the lake were primarily authigenic with only a minimal input from the lake catchment. These sediments contain a large quantity of Si(b) and Ca(a), as well as being rich in these two elements these sediments also contain a large quantity of CaCO₃ and organic material (see figure 9.1).

The first peak in X, between 166 and 146 cm is associated with the input of sediment from the catchment. The sediment chemistry suggests that both weathered

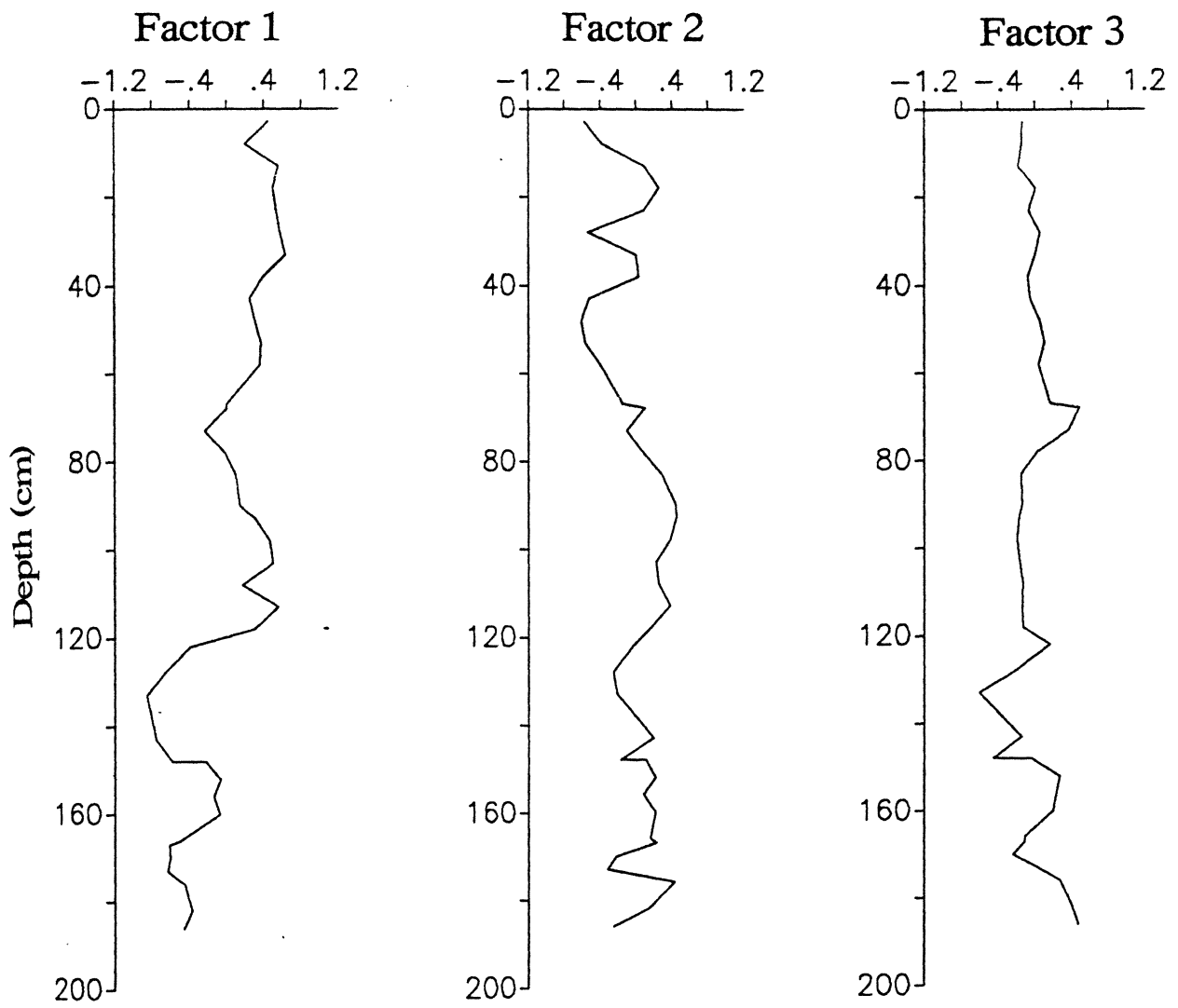


Fig. 9.4 Down-profile changes in factor loadings for LP11

and unweathered material was introduced into the lake at this time. Samples from this unit still indicate that Ca(a), Sr(a) and Mg(a) are very important in the chemical make up of this sediment.

Above 120 cm, the sediment chemistry record indicates a significant shift in the sediment source and confirms the results of the physical properties of the core. At this point in the core there is an increase in all those elements that indicate sediment input into the lake from the catchment. Between 120 and 80 cm sediments entering the lake were dominated by unweathered detrital sediment, although there is an increase in the quantity of weathered material entering the lake. While the input of unweathered material remains high throughout this part of the core, weathered sediment entering the lake decreases quite noticeably.

At about 80 cm there is a decline in all elements indicating the influx of clastic sediment into the lake. A decrease in the quantity of Ca(a) and Sr(a) is also noted. The most important chemical component of this part of the core designated **Zone V**, is Si(b) which suggests that during this period there were considerable algal blooms.

In the upper part of the core there is a sharp increase in the quantity of weathered material entering the lake. The amount of unweathered sediment although slightly higher than **Zone V**, is still very low. This suggests that during the most recent phase of erosion the majority of sediment coming into the lake in the early stages of sediment input was weathered sediment. In the upper part of the core there is an increase in the quantity of unweathered material entering the lake.

9.3 THE MASTERCORE (MC)

9.3.1 Sediment Chemistry

Seven stratigraphical zones can be identified in the upper 3.36 m of the MC, and these will be used to describe the salient features of the sediment chemistry record (Fig. 9.5). The most noticeable feature of **Zone I**, 336-316 cm, is the large peak in Al(c)

and Mg(c), and the abrupt reduction in the quantity of these two elements at the boundary of **Zone I** and **Zone II**. Fe(c), Si(c) and P(a) also display relatively high values in **Zone I**, increasing gradually to a peak at the boundary with **Zone II** (Fig. 9.5).

Zone II, 316-270 cm, is characterized by very large quantities of Si(b), which increases in amount up the zone. A small peak in Sr(a), Ca(a) and Mg(a) is observed at 280 cm which corresponds to slightly lower levels of Al(a), K(a), Zn(a) and Pb(a).

A large peak in Ca(a) and Sr(a) and a smaller peak in Mn(a) and Mg(a) are the main feature of **Zone III**; 270-220 cm. These elements all peak at approximately 250 cm, corresponding to a marked decrease in the amount of Fe(a), Ti(a), Al(a), Si(a), K(a), K(a), Si(b), Si(c), Fe(c), Ti(c) and Mg(c). As the amount of Ca(a), Sr(a), Mg(a) and Mn(a) decreases most other elements increase in value.

Zone IV, 220-180 cm, is characterised by large quantities of Fe(a), Ti(a), Al(a), Si(a), K(a), and Zn(a), at the base of **Zone IV**, but these elements decrease in value in the upper part of this Zone. At the top of **Zone IV** a small peak in Sr(a), Ca(a), Mg(a) and Mn(a) is noted.

A gradual increase in the level of Fe(a), Ti(a), Al(a), K(a), Zn(a), P(a), and Pb(a) as well as Al(c), Fe(c), Ti(c) characterises **Zone V**; 180-120 cm. In the upper part of the zone all these elements display a slight decrease in value with a corresponding increase in the amount of Ca(a) and Sr(a).

A distinct peak in Sr(a), Ca(a) and Mn(a) dominates the sediment chemistry record in **Zone VI** (120-90 cm). With the exception of P(a), which remains relatively unaltered, and Pb(a) which peaks markedly in the upper part of this zone, all other elements have lower values in this Zone.

Zone VII, 90-0 cm, is characterized by high levels of Fe(a), Al(a), Si(a), K(a), P(a), Ti(a) and Zn(a) which all increase in value up profile. Al(c), Ti(c), Fe(c), are found in quite high levels in the lower part of **Zone VII**, but are found in even greater quantities in the upper 40 cm of the core. Except for a small peak at 70 cm, Sr(a), Ca(a), Mg(a), and Mn(a) are all found in relatively low values in this Zone.

9.3.2 Correlations

There is a strong positive correlation between those elements that are believed to represent weathered detrital material Fe(a), Ti(A), Al(a), K(a), and Zn(a) (table 9.2). The strongest relationship in the data set is found between Ti(a) and K(a), $r=0.78$, Fe(a) and K(a), $r=0.77$, Ti(a) and Ti(c), $r=0.77$, Fe(a) and Ti(c), $r=0.72$ and Fe(a) and Ti(a), $r=0.68$. In addition, Fe(a), Ti(a) and Zn(a) correlate positively with Ti(c). The strongest correlation in this data set is between Mn(c) and Ca(c), $r=0.92$, however, these elements only occur in minute amounts in the sediment and are possibly associated with inputs in volcanic ash deposits. A strong positive relationship is also observed between Ca(a) and Sr, $r=0.85$. The levels of correlation in the MC are not as strong as those observed at LP11.

9.3.3 Factor Analysis

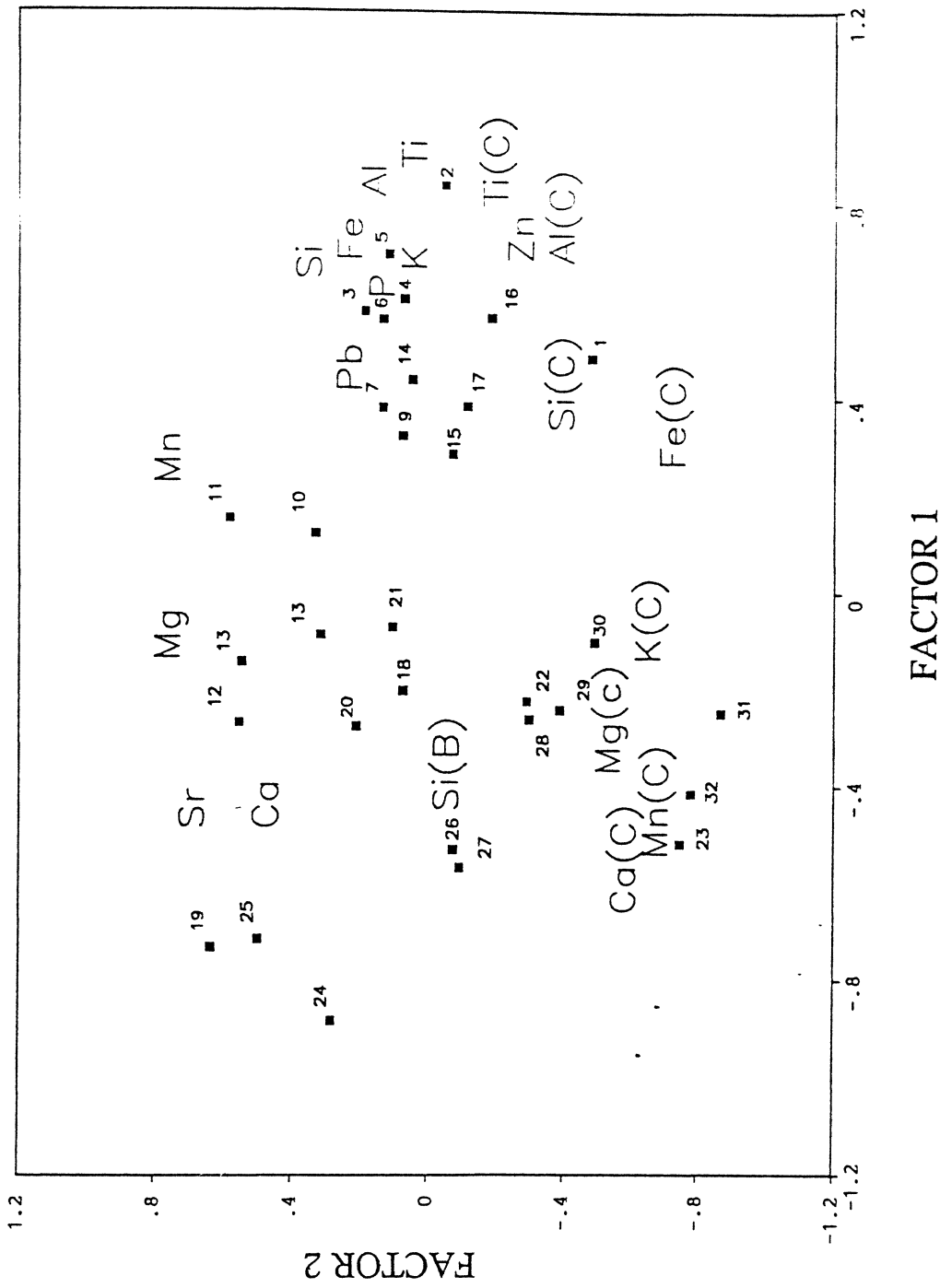
The Factor analysis on the upper 3.36 m of the Mastercore indicates that 67.4% of the variation within the core can be explained by the first three Factors. Factors 1, 2 and 3 account for 34.15%, 24.25% and 9% of the variation within the data set respectively.

The distribution of variables in relation to Factors 1 and 2 is seen in Figure 9.6. A number of distinct clusterings can be observed. A large number of variables load positively on Factor 1, however, it is possible to divide these variables into those that load positively and those that load negatively on Factor 2. In the case of the former group of variables there is a decrease in the loading on Factor 1 as the loading on Factor 2 increases. Thus, Ti(a), which loads strongly on Factor 1, barely influences Factor 2, while Cu(a) and Si(a), which load more positively on Factor 2, have a lesser control on factor 1. The second cluster of variables that load positively on Factor 1, but negatively on Factor 2, includes Ti(c), Al(c), Si(c) Fe(c) and Zn(a).

The distribution of samples on the plot of Factors 1 and 2 clearly indicates that certain sample groupings are associated with certain variables. In the case of Factor 1 it

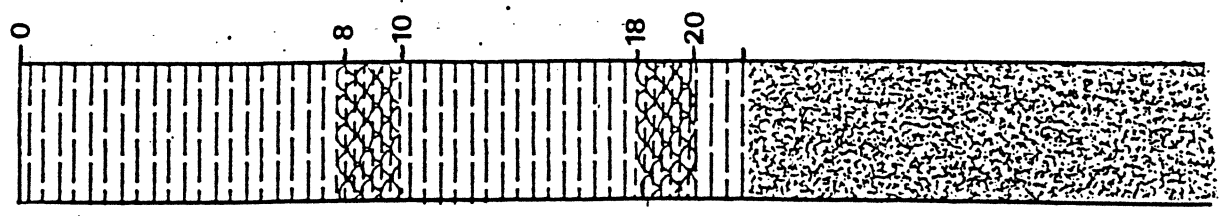
Fe(a)	Al(a)	Ti(a)	Mg(a)*	Mn(a)	Ca(a)	Al(a)	Si(a)
0.390							
0.670	0.603						
-0.151	-0.345	-0.171	0.698				
0.194	-0.186	0.129	0.331				
-0.216	-0.400	-0.305	0.302	0.302	-0.426		
0.506	0.308	0.600	0.052	0.378	-0.316	0.623	0.401
0.470	0.149	0.378	0.265	0.168	-0.319	0.556	-0.111
0.777	0.265	0.783	-0.056	0.490	0.853	-0.258	0.247
-0.284	-0.534	-0.461	0.617	-0.019	-0.453	0.574	0.456
0.532	0.501	0.747	-0.416	0.130	0.022	0.439	0.424
0.538	0.358	0.401	0.082	0.479	0.242	0.543	0.430
0.415	0.433	0.420	0.101	0.385	-0.335	0.574	-0.369
0.453	0.305	0.415	0.092	-0.366	0.083	-0.396	0.236
-0.375	-0.266	-0.290	-0.163	-0.240	-0.349	0.281	-0.139
0.087	0.449	0.141	-0.297	-0.377	-0.331	0.067	0.224
0.123	0.327	0.033	-0.631	0.194	-0.227	0.392	-0.270
0.715	0.567	0.768	-0.279	0.425	-0.212	0.154	-0.314
-0.163	0.253	-0.149	-0.316	-0.394	-0.174	-0.285	-0.370
-0.155	-0.026	-0.257	-0.295	-0.084	-0.084	-0.357	-0.203
-0.291	-0.153	-0.360	-0.233	-0.444	-0.255	-0.187	
-0.090	0.266	-0.180	-0.281				
K(a)	Sr(a)	Zn(a)	Cu(a)	P(a)	Pb(a)	Si(b)	Si(c)
-0.370							
0.587	-0.601			0.492	-0.276		
0.386	-0.061	0.295	0.260	-0.372	0.006	-0.231	0.502
0.336	-0.107	0.460	0.248	0.258	-0.062	-0.094	0.261
0.426	-0.111	0.283	0.248	0.208	0.321	-0.474	0.010
-0.298	0.001	-0.316	-0.312	0.437	-0.128	-0.014	0.193
-0.010	-0.409	0.370	0.219	-0.370	-0.206	-0.169	0.174
-0.003	-0.512	0.406	-0.163	0.208	-0.062	-0.069	0.227
0.565	-0.450	0.660	0.375	0.437	0.321		
-0.155	-0.243	0.074	0.261	-0.245	-0.128		
-0.301	-0.264	-0.235	-0.264	-0.321	-0.206		
-0.359	-0.164	-0.392	-0.274	-0.370	-0.273		
-0.186	-0.330	-0.069	-0.289	-0.225	-0.215		
Fe(c)	Ti(c)	Mg(c)	Mn(c)	Cu(c)			
0.312							
0.278	-0.148						
0.412	0.152	0.069					
0.322	-0.021	-0.033	0.923				
0.495	0.067	0.595	0.535	0.474			

Table 9.2 Correlation matrix from sediment chemistry data set from Mastercore



FACTOR 1

Figure 9.6 Distribution of samples and variables on Factors 1 versus Factor 2 for the Mastercore. Samples locations shown against core stratigraphy.



is evident that there is a very close link between Ti(a), Al(a), K(a), P(a), Fe(a), Si(a), Pb(a) and Cu(a) which constitute the weathered fraction of the material deposited into the lake from the catchment basin and samples taken from the upper two clay units (Fig. 9.6). Samples associated with the lower of these two units exhibit a strong connection with Ti(c), Al(c) Si(c) and Fe(c), suggesting that unweathered material is an important constituent of these samples. A similar relationship was noticed for LP11 and the MC. In addition, those samples that were taken from the upper clay unit tend to have a stronger association with those variables that indicate the input of weathered detrital sediment into the lake.

Those samples that load positively on Factor 2 appear to be closely associated with the variables Sr(a), Ca(a), Mg(a) and Mn(a). In all cases these samples were collected from ostracode-rich layers although as pointed out above those that were analysed from the uppermost unit are also influenced to a large extent by material entering the lake from the drainage basin, which in this instance is made up of the weathered fraction of material entering the lake. The remaining samples and variables load negatively on both Factors 1 and 2, however, this does not imply that there is a relationship between the two. This suggests that during deposition of the lower ostracode units there was little sediment entering the lake from the drainage basin, while during accumulation of the uppermost ostracode unit sediment from the drainage basin was entering the lake.

A small cluster of variables are seen to load negatively on both Factor 1 and 2 and include Mg(c), Mn(c), Ca(c) and K(c). Sr(a), Ca(a) and Mn(a) all load positively on Factor 2, with Sr(a) and Ca(a) loading negatively, Mg(a) plotting very slightly negative and Mn(a) being slightly positively on Factor 1. Si(b), Ca(c), Mg(c) and K(c) all load negatively on Factors 1 and 2.

The distribution of variable loadings for Factor 2 versus Factor 3 displays a large cluster in the central part of the plot, with a number of smaller clusters distributed around the main group. Sr(a), Mg(a) and Mn(a) all load very positively on Factor 2, and slightly

negatively on Factor 3. Fe(c) and K(c) both exhibit a strong negative loading on Factor 2 and slightly negative on Factor 3, while Ca(c) and Mn (c) both load together negatively on Factor 3 and Factor 2. The variable with the strongest influence on Factor 3 is Si(b) which as seen in Figure 9.7, has little influence on Factor 1 and none on Factor 2.

Distinct groups of samples and variables are not as easily distinguished on Factor 2 versus Factor 3. Most of the samples and variables cluster around the central part of the graph, although a distinct cluster of samples and variables can be seen to load positively on Factor 2.

The first three factors explain 34.14%, 14.25% and 9% of the variation in the core sediment data set respectively. When these are plotted against depth it is possible to determine which factors dominate sediment chemistry through time (Fig. 9.8). At the base of the core, however, those variables that load on Factor 3, dominate the sediment record, the most important of these variables being Si(b). The relative importance of Si(b) in this part of the core is confirmed by Bradbury (unpubl. data) which indicates quite high peaks in diatom concentrations with in excess of 1000 diatoms mm^{-2} at these levels. Other important peaks in diatom concentrations also coincide with peaks in the relative importance of Factor 3.

It is evident that there is a marked inverse relationship between Factors 1 and 2 thus where those factors that load on Factor 1 dominate the sediment record those that load on Factor 2 have little significance. The variables that load on Factor 1 are associated with detrital material and suggest instability within the drainage basin. Although weathered detrital material does load slightly positively on Factor 2 this factor is dominated by Sr(a), Ca(a) and Mg(a) which indicates more stable conditions in the basin.

9.3.4 Summary Of The Mastercore

The sediment chemistry record of the upper 3.36 m of the MC is not unlike that observed at LP11. At the base of the core large quantities of unweathered material are

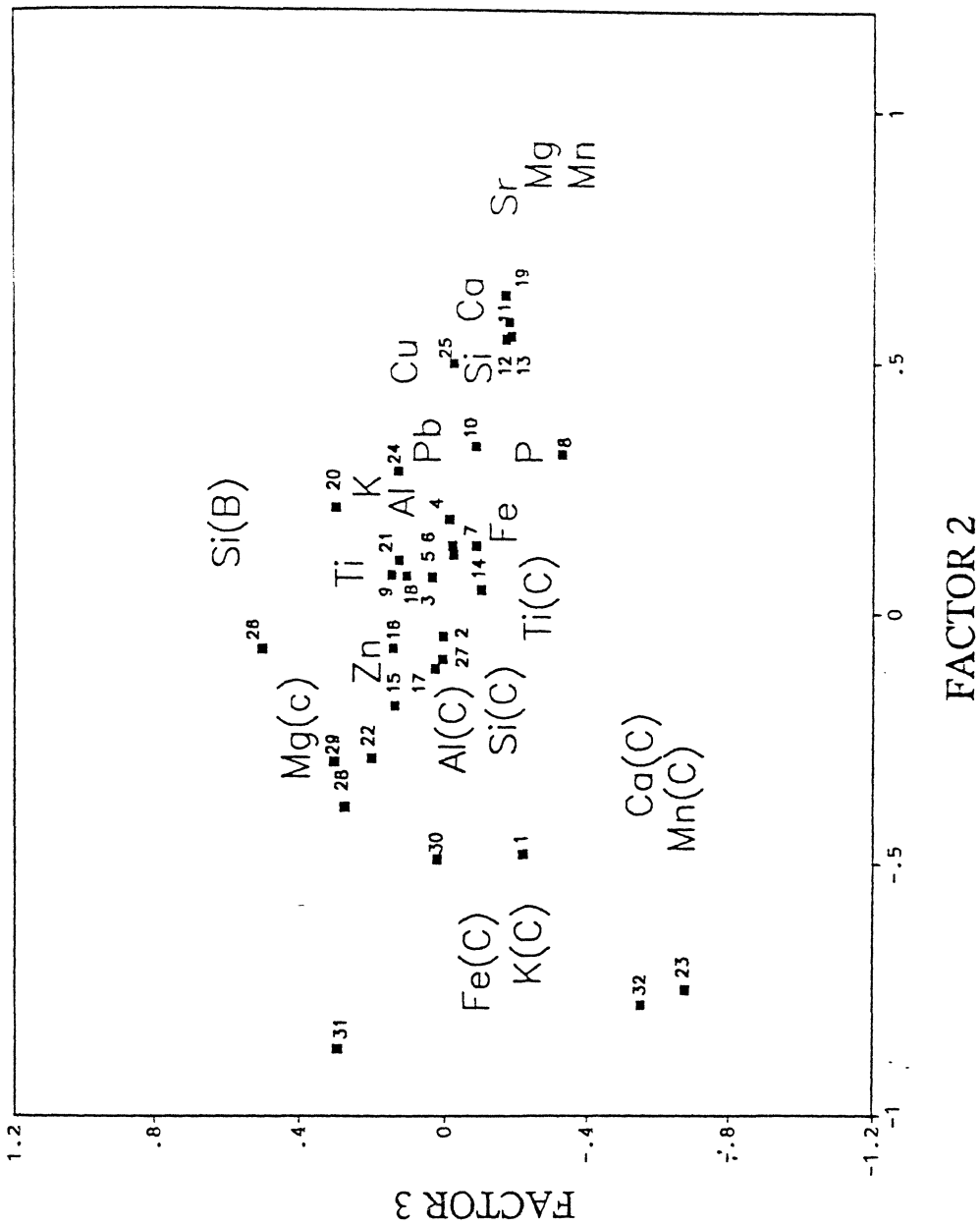
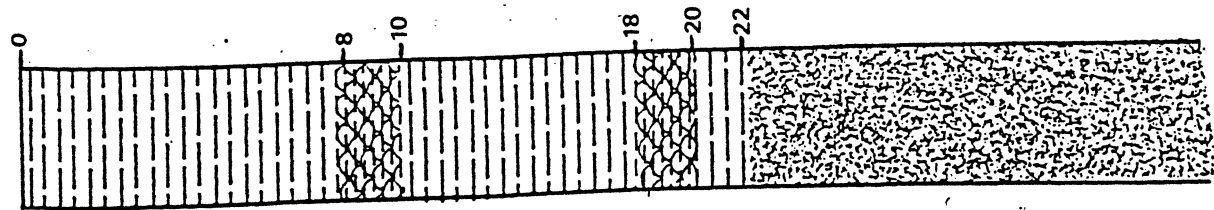


Figure 9.7 Distribution of samples and variables on Factors 2 versus Factor 3 for the Mastercore. Samples locations shown against core stratigraphy.



Factor 1

Factor 2

Factor 3

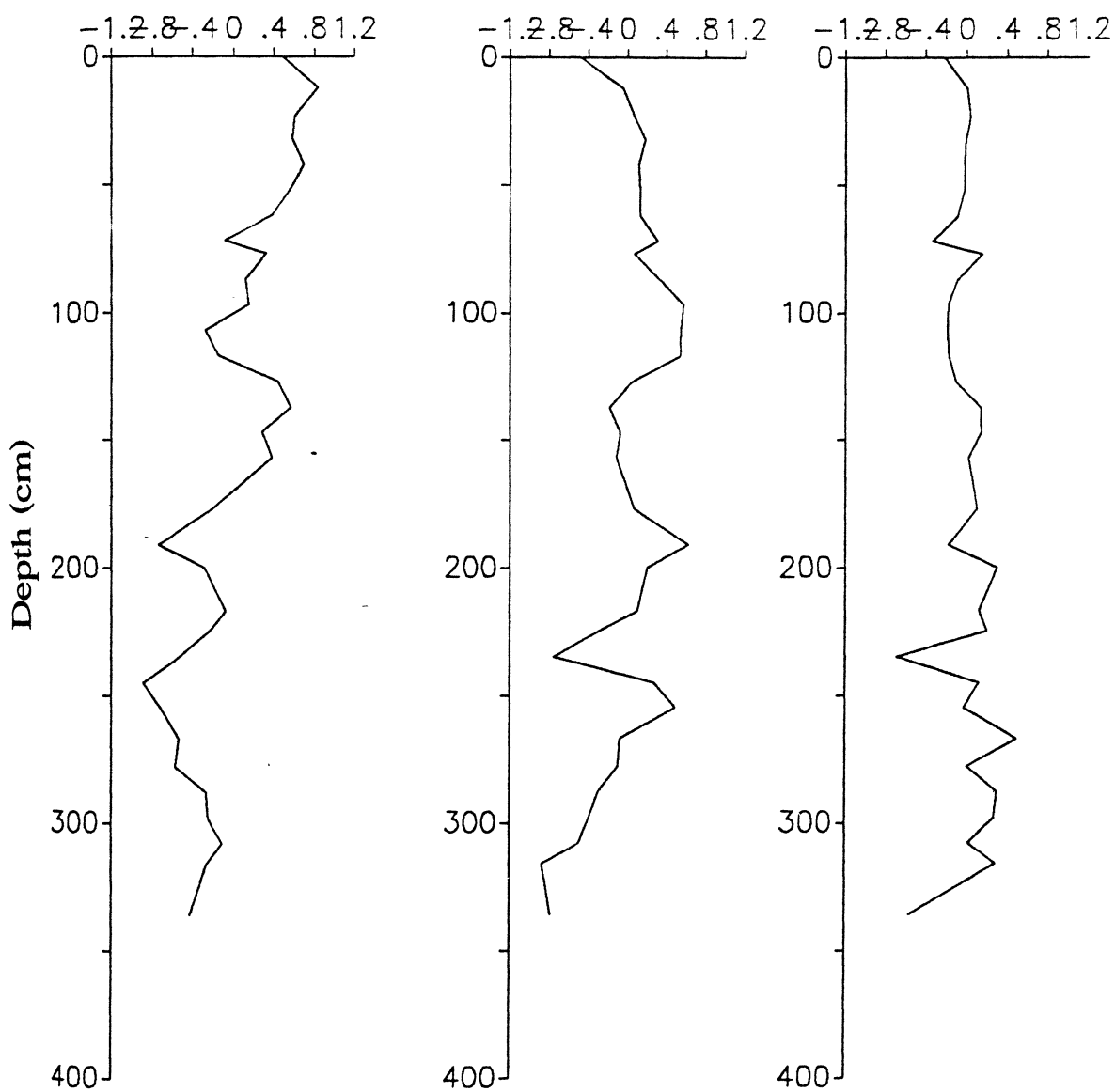


Fig. 9. 8 Down-profile changes in the factor loadings of the Mastercore

found which correspond to a small peak in X (Fig. 4.7). Between 316 and 220 cm the most important components of the sediments are Si(b) and Ca(a). These sediments also contain a large quantity of organic material. The sediment chemistry make up is very similar to that at LP11. Above 220 cm there is a dramatic change in the sediment chemistry with a huge increase in those elements extracted in the 'a' fraction associated with weathered clastic sediment. There is a noticeable decrease in the input of unweathered material entering the lake at this time.

At 180 cm there was a dramatic increase in the amount of sediment entering the lake from the drainage basin. Unweathered sediment in particular dominates this material. Through this period there is a decrease in the amount of biogenic silica.

In the upper 180 cm of the MC the sediment chemistry is dominated by material entering the lake from the catchment. In **Zone V**, there is an increase in Fe, Ti and Al and K extracted in both the 'a' and 'c' fractions, all indicating instability within the basin: unweathered material forming the bulk of sediment entering the lake. Samples from this part of the core clearly display a close association with the unweathered fraction in the factor analysis. Only between 100 and 70 cm where sediments are rich in ostracodes is there a reduction in the amount of material entering the lake.

9.4 LAKE PATZCUARO 10

9.4.1 Sediment Chemistry

Four main zones can be distinguished from LP10, this zonation being based on stratigraphical and X variations (Fig. 9.9). The main feature of **Zone IV**, 190-165 cm, is the small peak observed in Al(a), Ti(a), Fe(a), Zn(a), K(a), Mn(a), Si(a), Ti(c) and K(c). All these elements are found in much lower amounts in the upper part of this Zone. There is a drop in the values of Fe(c), Al(c) and Si(c) in the upper part of **Zone IV** as well. P(a), and Mg(a) display an inverse relationship to this with a slight peak noted in the upper part of **Zone IV**, a similar peak in Sr(a), and Ca(a) is also noted. Si(b) is found in large

quantities throughout Zone IV.

Zone V, 90-165 cm, is characterised by very low levels of Ca(a), Sr(a) and Mg(a). The curves for Al(a), Fe(a), Zn(a), K(a), and Si(a) are all very similar, exhibiting relatively high values throughout the zone although there is a slight decrease in all values at approximately 120 cm concomitant with a slight peak in Fe(c).

A relatively large peak in Ca(a) and Sr(a) as well as high levels of Mg(a), and P(a) typify **Zone VI**, 60 to 90 cm. It should be noted that the peaks in the latter two elements are slightly further up profile than the former two elements. All other elements are found in relatively low amounts in this part of the core, although there is a slight peak in those elements extracted in the 'C' fraction in the upper part of the Zone prior to dropping to lower levels at the boundary of **Zones VII and VII**.

Ca(a), and Ca(a) maintain low values in the upper 60 cm of LP10, **Zone VII**, with slightly higher levels of Al(a), Ti(a), Fe(a), Zn(a), and K(a). In the case of Fe(c), Al(c), Ti(c) and K(c) there is a marked increase in the relative value of these elements in the upper 50 cm of the core.

9.4.2 Correlations

The correlation matrix for the sediment chemistry data set from LP10 is shown in Table 9.3. A very strong positive correlation is found between Fe(c), Al(c) and Ti(c). Between Al(c) and Ti(c), $r=0.94$; Al(c) and Fe(c), $r=0.92$ and Ti(c) and Fe(c), $r=0.93$. A very strong positive relationship is also found between Ca(a) and Sr(a), $r=0.91$. Both Ca(a) and Sr(a) also display a strong positive correlation with Mn(a), $r=0.74$ and $r=0.82$ respectively. A strong negative relationship is noted between Si(b) and elements extracted in the 'c' fraction, in particular, Al(c) $r=-0.69$, Ti(c) $r=-0.67$ and Fe(c) $r=-0.65$.

9.4.3. Factor Analysis

Factor analysis was run on only twenty samples from core 10. Due to the limited number of samples it was necessary to carry out the analysis on a slightly reduced data

Table 9.3 Correlation matrix from sediment chemistry data set from LP10

	Fe(a)	Ca(a)	K(a)	Mn(a)	Al(a)	Sr(a)	P(a)	Ti(a)
	-0.455							
	0.550	-0.144						
	0.023	0.737	0.156					
	0.521	-0.493	0.140					
	0.271	-0.324	0.045	-0.327	0.257			
	-0.333	0.076	-0.428	-0.004	-0.215	-0.264		
	0.517	-0.411	0.379	-0.051	-0.013	-0.422	0.003	-0.427
	0.445	0.062	-0.276	-0.275	-0.157	-0.004	0.007	0.517
	0.452	-0.459	0.415	-0.298	0.742	0.413	-0.147	-0.310
	-0.513	-0.167	-0.257	-0.370	0.123	0.266	0.002	0.421
	0.618	-0.060	0.285	0.130	0.013	-0.249	-0.012	0.530
	0.633	-0.017	0.251	0.102	0.111	-0.097	-0.052	0.421
	0.496	0.060	0.315	0.132	-0.166	-0.363	-0.076	0.470
	-0.333	0.076	-0.469	-0.004	-0.215	-0.264	1.000	0.003
	0.617	-0.411	0.379	-0.051	-0.013	-0.422	0.003	1.000
	-0.222	-0.032	-0.098	-0.051	0.076	0.004	0.122	-0.113
	-0.510	0.028	-0.100	-0.291	-0.091	0.134	-0.040	-0.534
	0.154	-0.074	-0.045	-0.204	-0.107	-0.225	0.132	0.222
	-0.377	0.312	-0.084	0.817	-0.395	-0.157	0.071	-0.455
	Mq(a)	Zn(a)	Si(b)	Al(c)	Ti(c)	Fe(c)		
	-0.444							
	0.261	0.072						
	-0.166	0.173	-0.694					
	-0.108	0.158	-0.670	0.538	0.916	0.927	-0.076	
	-0.070	-0.004	-0.653	0.916	0.927	0.927	-0.076	
	0.007	-0.147	0.002	-0.012	-0.052	-0.052	0.490	
	-0.427	0.517	-0.310	0.530	0.421	0.421	0.490	
	0.413	0.070	0.247	-0.086	-0.089	-0.089	-0.179	
	0.813	-0.325	0.375	-0.255	-0.256	-0.256	-0.206	
	0.547	-0.198	-0.251	0.407	0.567	0.567	0.590	
	-0.005	-0.582	-0.166	-0.163	-0.108	-0.108	-0.077	
	Si(c)	Cu(c)	Mn(c)					
	0.454							
	0.074	0.117						
	0.005	0.084	-0.260					

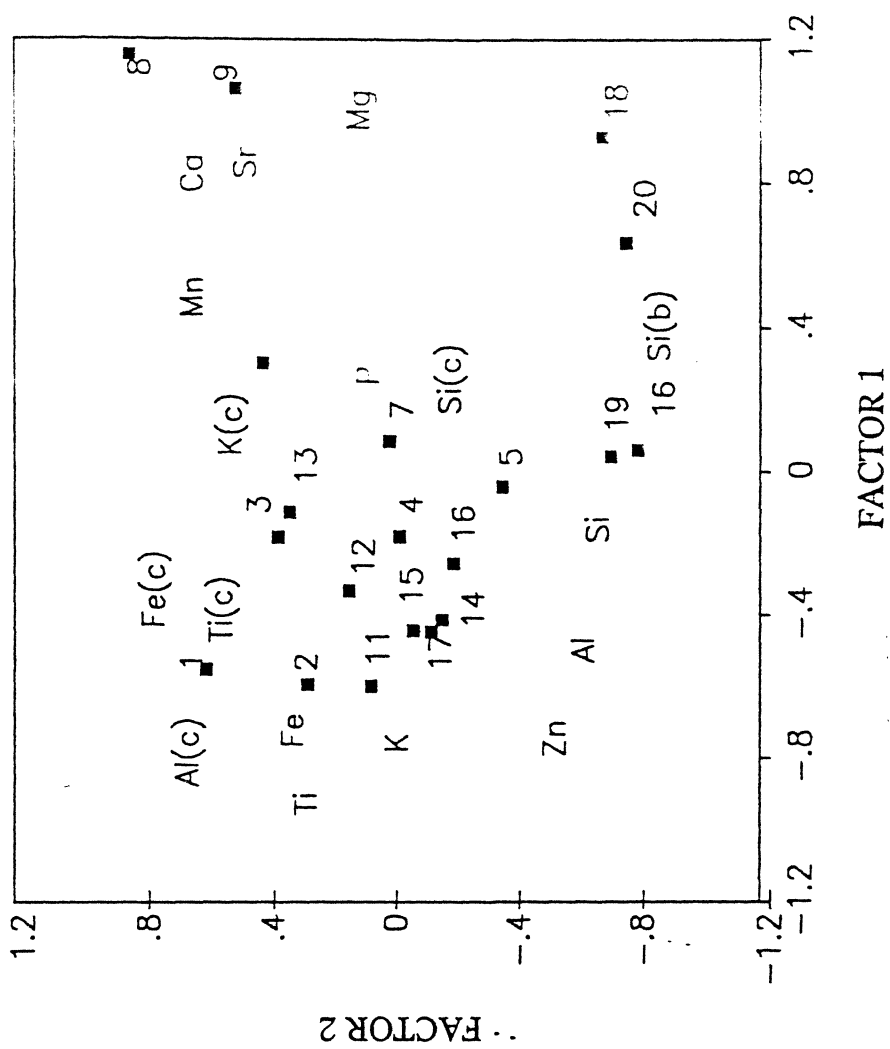
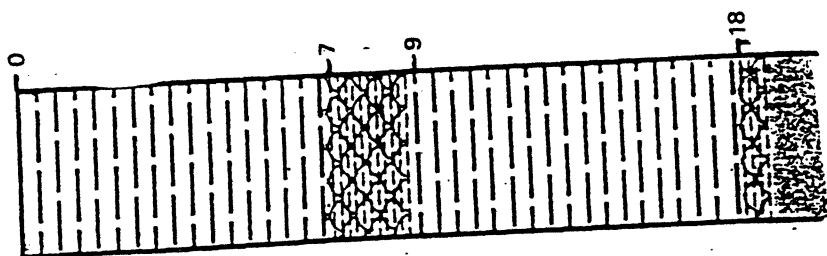


Figure 9.10 Plot of variables and samples on Factor 1 versus Factor 2 for LP10 showing stratigraphy and position of sample



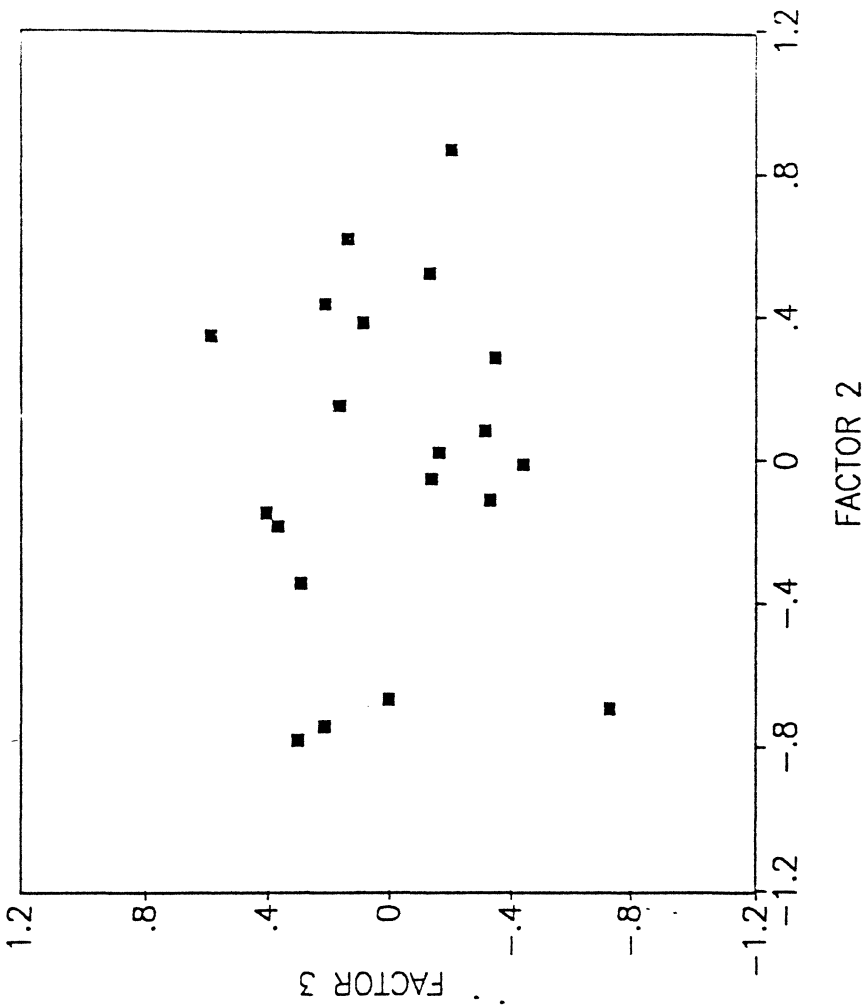
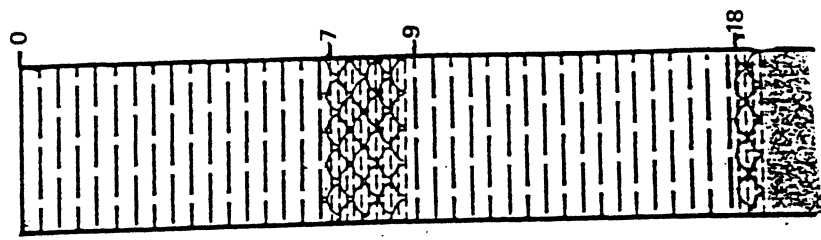


Figure 9.11 Distribution of samples and variables on Factors 2 versus Factor 3 for LP10. Samples locations shown against core stratigraphy.



set as the number of variables has to be smaller than the number of samples for the programme to run (Walden, 1990). In this instance it was believed that Ca(c) formed a relatively insignificant level in the core and thus was not analysed in the data set.

There is a wide distribution of the variables and samples on the plot of Factor 1 versus Factor 2 (Fig. 9.10). Mg(a) loads very strongly on Factor 1, as do Sr(a) and Ca(a). The latter two variables also show a strong positive loading on Factor 2. A large number of variables load negatively on Factor 1. These include Al(c), Fe(c), Ti(c), Ti(a) and Fe(a). Ti(c), Fe(c) and Al(c) also display show a strong positive loading on Factor 2. Zn(a), Al(a) and Si(a) all load negatively on both Factors 1 and 2.

The majority of samples from LP10 load negatively on Factor 1, plotting in a loose cluster both slightly negatively and positively on Factor 2. Only four of the twenty samples plot away from this main group, samples 8 and 9 load positively on Factors 1 and 2 and plot very closely to Sr(a) and Ca(a). Samples 18 and 20 exhibit a strong positive loading on Factor 1, but loads very negatively on Factor 2 and are closely associated with Si(b). The majority of samples, however, are closely related with Al(c), Fe(c), Ti(c), Ti(a), Fe(a) Zn(a) and Al(a). This relationship indicates that the sediment is dominated by material entering the lake from the catchment both in a weathered and unweathered form.

The plot of Factor 2 versus Factor 3 (Fig. 9.11) exhibits the fact that a large number of variables plot positively on Factor 2. Displaying the strongest positive loading are Fe(c), Ti(c) and Mn(a) with Al(c), Sr(a) and Ca(a) also displaying a positive loading on Factor 2.

What is evident from Figure 9.11 is that the majority of samples from the upper part of the core (ie. that are associated with the upper two clay units and the ostracode rich sediment layer) are strongly influenced by those variables that indicate influx of detrital material into the lake. In comparison samples from below these units plot in positions that would indicate little influence from detrital material.

The variables that load on Factor 1 (Fig. 9.12) and explain 29.8% of the variation

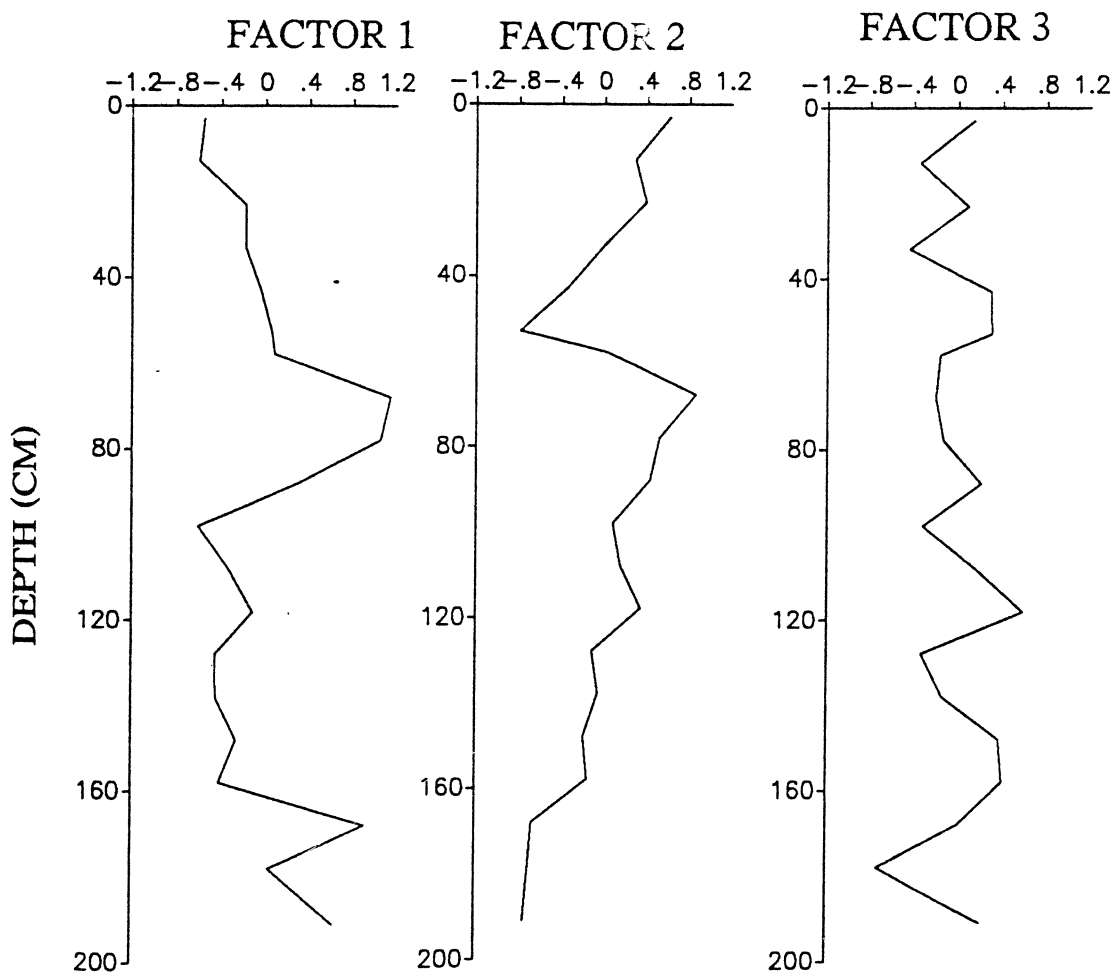


Fig. 9.12 Down-Profile changes in the factor loadings for LP10

in the data set are Mg(a), Ca(a), Sr(a) and to a certain extent Mn(a) and Si(b). However, it is only in two parts of the core that these dominate the sediment chemistry record, these being at the base of the core and between 95-60 cm (Fig. 9.12). Elsewhere these variables display a very negative loading.

In the case of Factor 2 which accounts for 22.86% of the variation the most important variables are Fe(c), Al(c) Ti(c), Ca(a), Sr(a) and Mn(a). The importance of these variables on the sediment chemistry record shows a marked increase from the base of the core up to approximately 60 cm, with a sharp negative peak at 52 cm. From this point to the top of the core there is a gradual increase in the importance of variables loading on this factor.

A much lesser degree of variation is observed for the plot of Factor 3 (Fig. 9.12) and although it accounts for only 7.6% of the variability of the data set only P and Ti show any degree of positive loading.

9.4.4 Summary of Lake Patzcuaro 10

It is evident from the geochemical analysis of LP10 that the sediment chemistry is dominated by material that has entered the lake from the catchment in both a weathered and unweathered form. These results confirm those of the investigation into the physical properties of the sediment. At the base of the core Si(b) is one of the most important constituents of the sediment make up, but becomes progressively less so up the core.

In the lower erosional event sediment make-up is divided between weathered and unweathered material in the lake. At the base of the uppermost phase there is a noticeable change in the sediment chemistry. The base of the unit is characterised by more weathered material entering the lake. In the upper 40 cm of the core, however, there is a marked increase in the amount of unweathered sediment entering the lake at LP10.

This relationship is similar to that observed at the MC and LP11. The distribution of samples indicates that no factor really dominates the sediment record.

There is a gradual decrease in the amount of Si(b) in the sediment record which indicates a reduction in diatoms possibly associated with the turbid conditions reducing light penetration and reducing species. Factor 1 explains 29.9% of the variability in the data set at LP10. The variables displaying the strongest positive loading on Factor 1 being Ca(a), Sr(a) and Mg(a) with Mn(a) and Si(b) exhibiting a lesser positive loading.

9.5 LAKE PATZCUARO 19

9.5.1. SEDIMENT CHEMISTRY

Five main zones can be delimited in LP19 and provide the basis for describing the salient features of the sediment chemistry record (Fig. 9.13). **Zone III**, 240-220 cm, is characterised by relatively high levels of Fe(a), Al(a), K(a), Mn(a), Si(b) as well as, Si(c), Fe(c), Al(c), K(c), and Mn(c). Low values of Cu(a), Sr(a), Mg(a), and Ca(a) are found in this part of the core.

A very large peak in Sr(a) and Ca(a) characterises **Zone IV**, 220-210 cm). This corresponds to slightly lower values of Fe(a), Al(a), Ti(a), Cu(a), K(a), Fe(c), Ti(c) and Al(c). Si(a) displays a gradual decline through this part of the core while Si(c) exhibits a small sharp peak at the boundary of **Zones III and IV** before dropping to lower values; K(c) displays a similar trend.

The most important feature of **Zone V**, 210-155, is the marked increase in Fe(a), Al(a), Ti(a), Mn(a), Cu(a), K(a), Mg(a) and Si(a) at the boundary of **Zones IV and V** (approximately 210 cm). However, the curves relating to these variables show quite considerable variations up in this zone with a large number of small peaks and troughs observed. In general these curves exhibit a similar pattern. A very sharp increase in the amount of Fe(c), Si(c), Al(c), and Mn(c) is also noted at the boundary of **Zone IV and V** peaking at 200 cm, before dropping to much lower levels and remaining as such throughout **Zone V**.

The most distinct feature of **Zone VI**, 145-155 cm, are large peaks in Sr(a),

Ca(a), and Mg(a). In marked contrast there is a marked decrease in the level of Fe(a), Al(a), Ti(a), Fe(c), Al(c), K(c) and Mn(c).

The upper 145 cm of the core is designated **Zone VII** and is characterised by a very 'noisy' signal with numerous small peaks and troughs. What is noticeable from this data set is that the curves for Fe(a), Al(a), Ti(a), and Mn(a) exhibit an inverse relationship to these elements extracted in the 'c' fraction. With the exception of a small peak at 130 cm the levels of Ca(a), Sr(a) and Mg(a) remain very low in this zone.

9.5.2. Correlations

The correlation matrix for the sediment chemistry data set from LP19 is shown in Table 9.4. A number of elements display a very strong positive relationship, in particular : Fe(a) and Ti(a), $r=0.91$; Fe(a) and Al(a), $r=0.86$; Al(c) and Ti(c), $r=0.84$; Al(a) and Ti(a), $r=0.83$; Fe(c) and Al(c), $r=0.82$ and Fe(c) and Ti(c), $r=0.79$. A strong positive relationship is also noted between Ca(a) and Sr(a) $r=0.74$. Both Ca(a) and Sr(a) also correlate positively with P(a) and Si(b) (Table 9.4). Despite the strong positive relationship displayed by the elements outlined above few other elements within the data set display such a clear negative or positive relationship as these variables.

9.5.3 Factor Analysis

The variable loadings for Factors 1 and 2 are shown in Figure 9.14. Three distinct groups can be distinguished together with a number of variables that appear to load independently of one another. Fe(c), Al(c) and Ti(c) exhibit a strong positive loading on both Factors 1 and 2. In comparison Ti(a), Al(a) and Fe(a) load positively on factor 1 but negatively on Factor 2. Displaying a very negative loading on factor 1 and having little influence on factor 2 is a group of variables consisting of Sr(a), Ca(a), Si(b), Si(c) and K(c).

It is evident from figure 9.14 that a large number of samples cluster together, all loading slightly positively on Factor 1, although these distribute both positively and

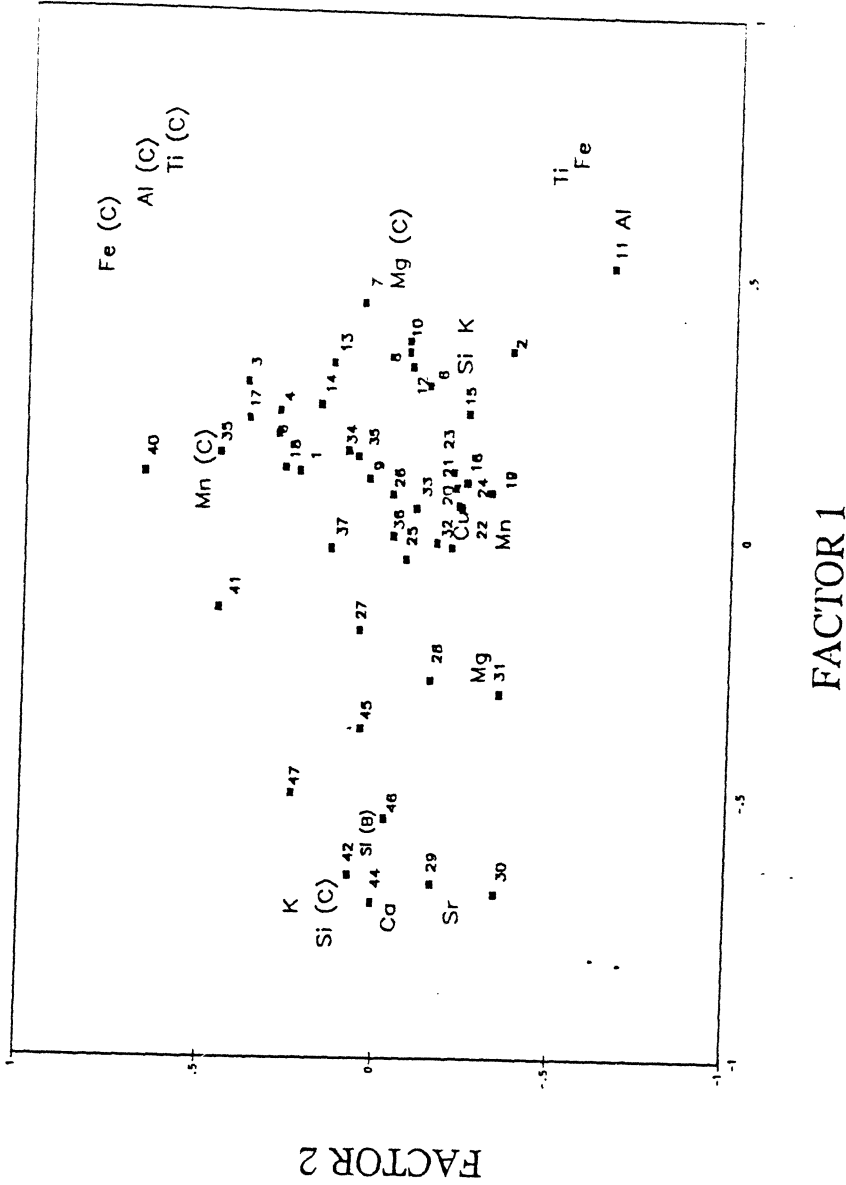
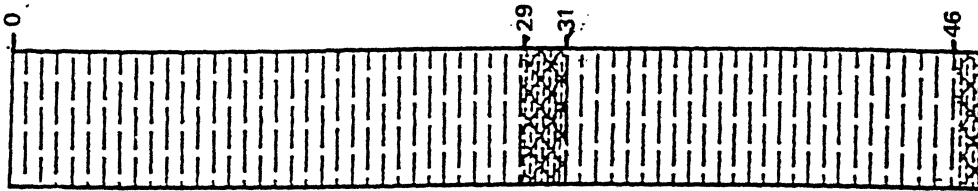


Figure 9.14 Distribution of samples and variables on Factors 1 versus Factor 2 for LP19. Samples locations shown against core stratigraphy.

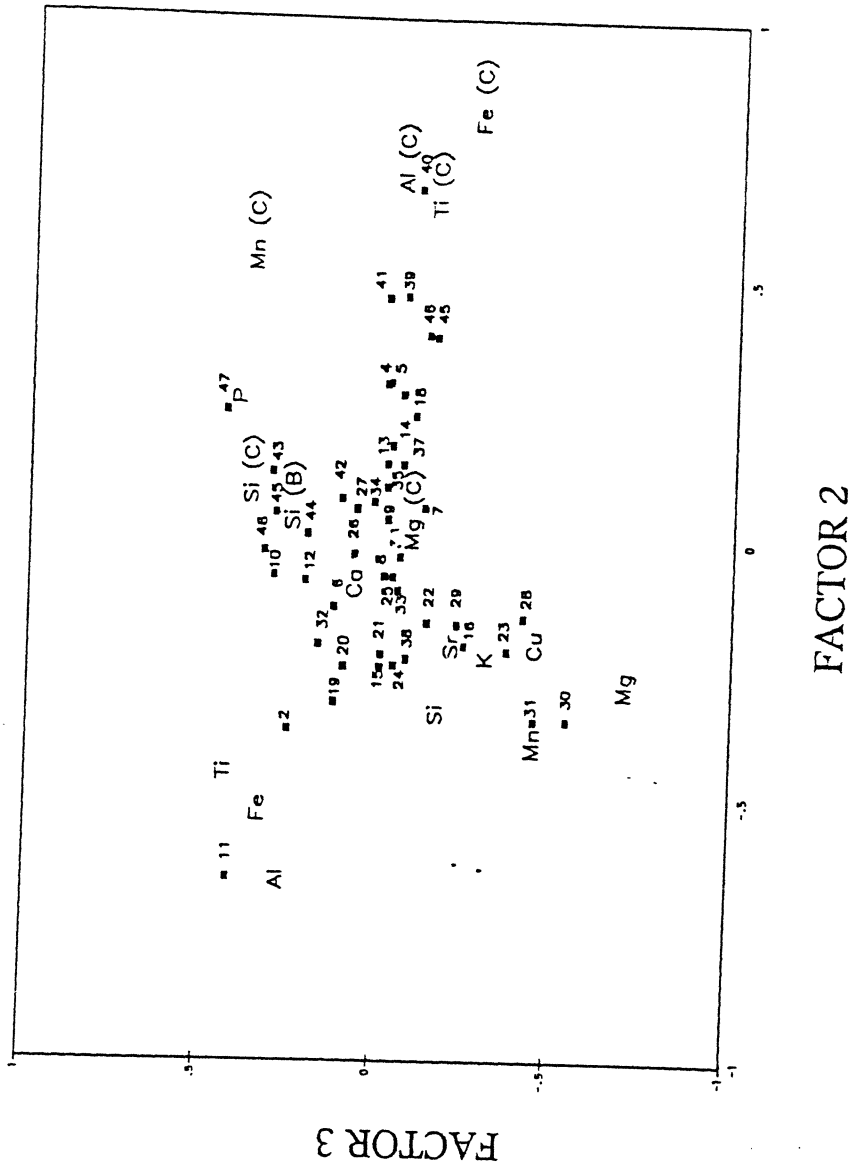
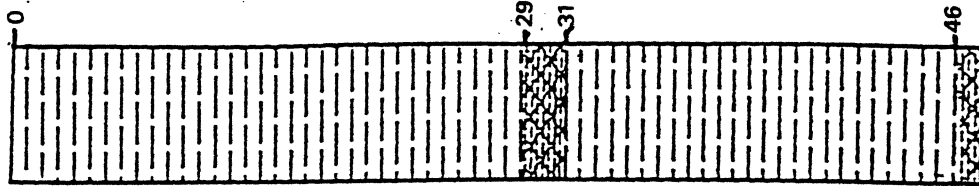


Figure 9.15 Distribution of samples and variables on Factors 2 versus Factor 3 for LP19. Samples locations shown against core stratigraphy.

negatively on Factor 2. A second group of samples that do not show the same degree of clustering load negatively on Factor 1. It is notable, however, that even on the two most important factors the overall distribution of samples is not very great. This would indicate that much of the sediment making up this core is very similar in chemical content.

In the case of Factor 1 versus Factor 2 it is apparent that the main grouping of samples that loads positively on Factor 1 is not influenced by any one group of variables. However, a small number of samples have similar loadings to Sr(a), Ca(a), Si(B), Si(c) and K.

Several much more distinct variable groupings can be identified from the plot of factor 2 versus factor 3. Al(c), Ti(c) and Al(c) reveals a very high positive loading on factor 2, but has little influence on factor 3. In comparison Al, Fe and Ti display a strong negative loading on Factor 1, but load slightly positively on factor 2. A further group of variables which appear not to have much control over Factors 1 and 2 consists of Ca(a), Mg(c), Si(B), Si(c) and P, while Si, Sr, K Mn, Cu, and Mg form a general cluster of variables that load negatively on both Factors 2 and 3.

The plot of Factors 2 and 3 (Fig. 9.15) shows a large number of samples cluster around the central part of the graph with a number drawing off from the main group towards major sample clusters. This suggests that these variables have a greater influence over these samples, although on the whole no one major group dominates the sediment chemistry.

The down-profile variations in the factor loadings are shown in Figure 9.16. Factor 1, which is associated with Al(a), Fe(a), Ti(a), K(a), Si(a), Mg(c), Ti(c), Al(c) and Fe(c), accounts for 30% of the variation in the data set. The curve is very similar to that of magnetic susceptibility (see Fig. 8.4).

Factors 2 and 3 which account for 22% and 7% of the variability of the data set are associated with unweathered and weathered clastic material respectively. There is a weak inverse relationship between these two factors and suggests periods when weathered or unweathered material dominate the sediment influx. Factor 2 is particularly

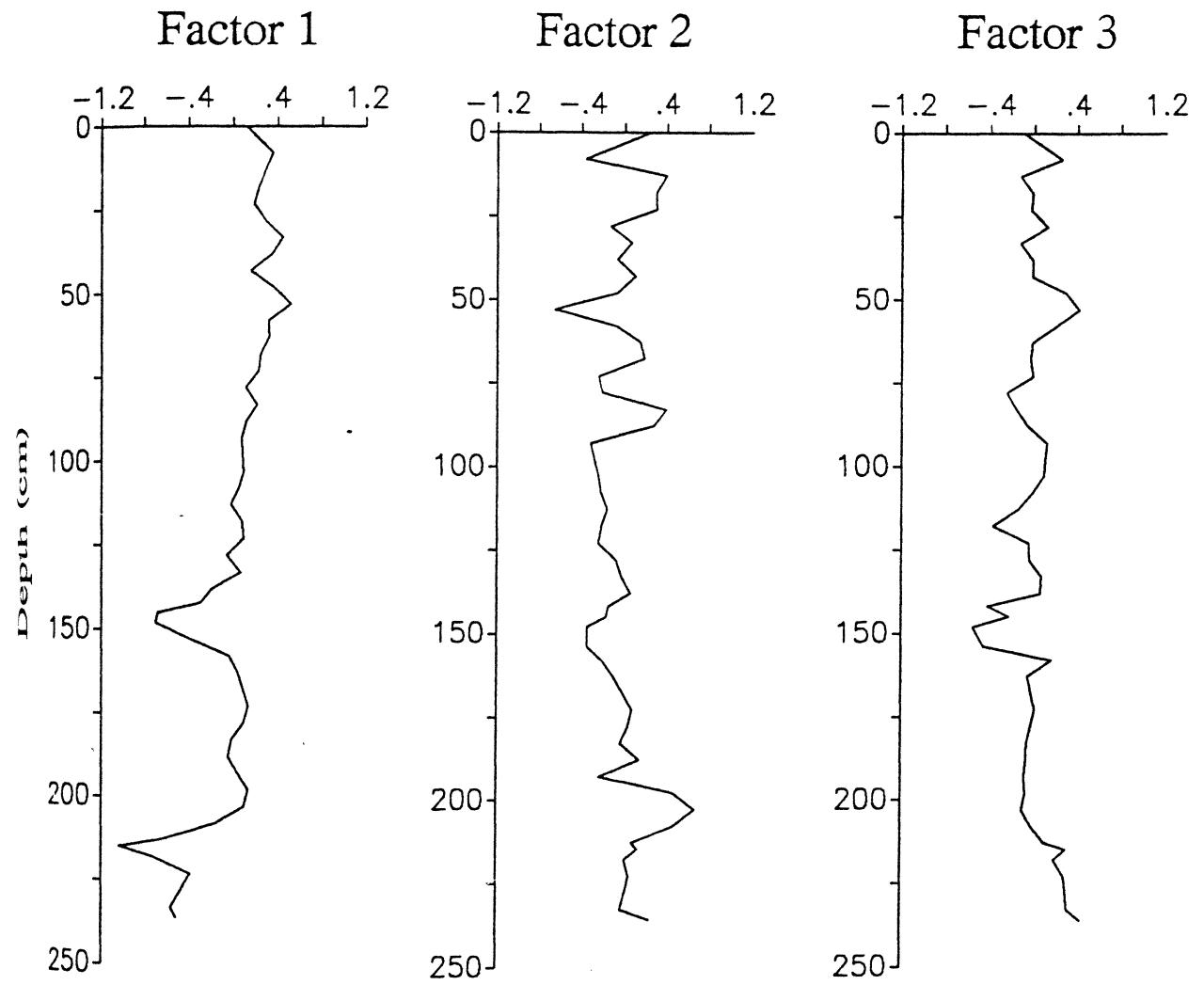


Fig. 9.16 Down-profile changes in factor loadings for LP19

important in the lower part of the core and in the upper 100 cm.

9.5.4 Summary Of Lake Pátzcuaro 19

It is evident from the results of the sediment chemistry analysis that the sediments at LP19 are dominated by material input from the catchment into the lake. These results confirm the conclusion based on the physical properties. Sediments at the base of the core are relatively organic rich and contain a relatively large amount of Si(b). At the base of Zone IV there is evidence of a considerable influx of unweathered material into the lake with a corresponding dramatic decrease in the amount of Si(b). The amount of weathered material decreases sharply above this initial influx of sediment.

In the upper part of the core the sediment chemistry record implies influxes of weathered and unweathered material. It does appear that there is a general increase in the amount of unweathered material entering the lake upwards through the core profile.

9.6 SUMMARY OF THE SEDIMENT CHEMISTRY RECORD OF THE LAKE PATZCUARO

In this section the main features of the sediment chemistry record of Lake Pátzcuaro will be summarized.

Only the upper part of Zone I was analysed in this part of the investigation. Sediments associated with this zone are characterised by peaks in the input of unweathered sediment. These elements may be associated with the input of unweathered volcanic material into the lake.

Identified at both LP11 and the MC, Zone II, displays peaks in Ca(a) and Sr(a); levels of Si(b) are also high. The increase in the concentration of these elements, especially Ca and Sr, probably reflects lower lake levels at this time. Sediments associated with Zone III are characterised by high levels of those elements that indicate the input of detrital material into the lake.

Large peaks in Sr and Ca are the main characteristic of Zone IV. The increase in the level of these elements suggests a lowering of the level of the lake at this time, Other

elements, in particular those that indicate sediment influx into the lake, display a marked decrease during the accumulation of these deposits.

Zone V is characterised by large peaks in all those elements that indicate influx of detrital material into the lake. It is quite apparent that with the exception of LP10 all the sediment chemistry records from the other core sites indicate that the material entering the lake contained a large quantity of unweathered material.

A marked decrease in detrital sediment input and peaks is the main feature of **Zone VI**. Peaks in Ca(a) and Sr(a) at all the cores except LP11 are also noted. In the case of LP11 an enormous peak in Si(b) is observed. Input of detrital sediment into the lake resumed in **Zone VII**. At all cores it is apparent that in the basal part of this zone, sediment entering the lake is dominated by weathered material with increasing quantities of unweathered material entering the lake in the upper part of this zone. **Zone VII** is also characterized by low Ca and Sr values although a slight increase is noted in the upper part of LP11.

Despite differences in the actual concentration values of different elements analysed it is apparent that the overall sediment chemistry record from Lake Pátzcuaro is broadly similar across the lake. Based on this evidence it is possible to determine periods of influx of sediment into the lake and the nature of the material that has accumulated at different times. Attempting to infer climatic changes from these data is not so easy, however. As discussed above the data presented here are in concentration units, and changes in the value of any one element will have a direct effect on the concentration of all other elements. Thus, peaks in Ca(a) and Sr(a) would occur when there is a decrease in the input of detrital material. Consequently peaks in Ca(a) and Sr(a), which were believed to be indicative of lower lake levels and hence drier climatic conditions, may not be as simple as it would seem. To determine conclusively whether or not these conditions are dry it would be necessary to determine the variations in the actual influx of different elements, however, this would require a considerably greater number of dates than are currently available on these cores.

9.7 CHANGES IN THE RATE OF SEDIMENT INFLUX INTO THE LAKE OVER THE LAST 3,500 YEARS.

The lacustrine record clearly provides the most detailed evidence of changes in erosion rates within the basin. This is due to the large quantity of cores available, distinct stratigraphical changes and excellent dating control. Using these data it is possible to estimate spatial and temporal variation in the rate of sediment influx into the basin.

There are various methods for calculating sediment accumulation rates in lakes. Studies that have been based on multiple cores frequently use contouring to determine the volume of sediment that has accumulated in a given time period (eg. Bloemendal, 1982; Dearing et al., 1981) Lake Pátzcuaro, however, is not suitable for this method of analysis due to its irregular shape and the considerable variations in the thickness of stratigraphical units found in different parts of the lake. Another method of calculating sediment influx is to divide the lake into a series of polygons, each associated with a core site. The characteristics of the core are assumed to be the same for the entire polygon.

Lake Pátzcuaro was divided into 21 polygons following the method outlined in Chapter 5 (Fig. 9.17). To determine the amount of sediment which has accumulated at each cores site for a given layer the following formula was applied:

$$\text{Layer thickness} \times \text{bulk density} \times \% \text{ clastic material}^*$$

The % clastic material was calculated using the following formula:

$$\% \text{ clastic} = 100 - (\% \text{ CaCO}_3 + \% \text{ L.O.I.} + \% \text{ SiO}_2)$$

As it is not possible to determine the amount of CaCO₃, organic matter and biogenic silica which may have been transported to the lake from the catchment it is assumed that the entire content within the core is a product of the lake itself. Only three units were identified throughout the entire lake which correspond to **Zone V**, **Zone IV** and **Zone VII**. The following results relate to these zones.

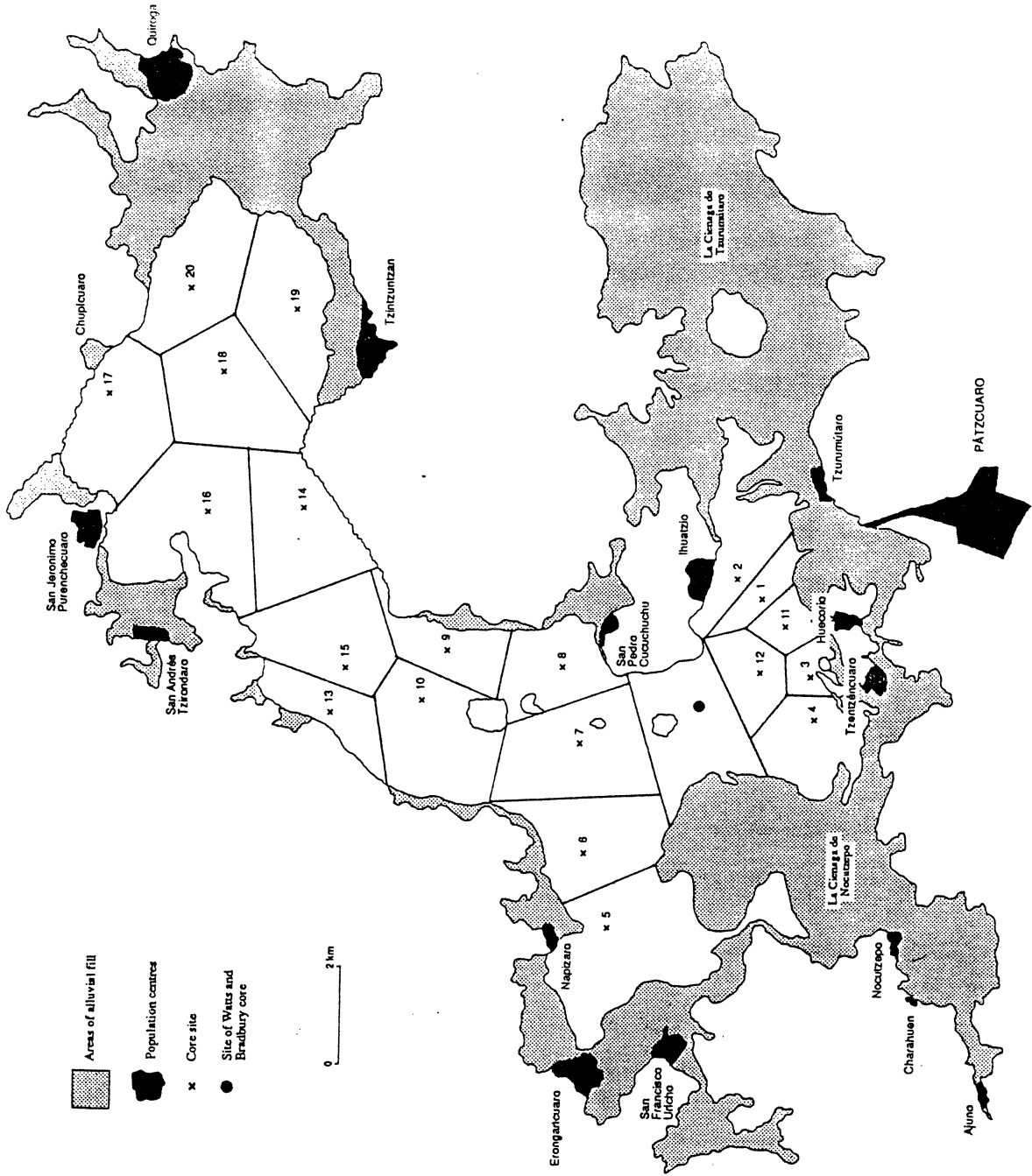


Figure 9.17 Lake Pátzcuaro divided into polygons that were used for determining sediment accumulation rates

9.7.1 Zone V (2,500-1,200 years B.P.).

Sediments associated with **Zone V**, accumulated during the second phase of erosion within the basin. These deposits were found at all the core sites analysed, and thus, it is possible to assess spatial variation in the quantity of sediment influx into the lake. The results of the analysis are shown in Table 9.5. There was a considerable difference in the amount of sediment input into the lake during the accumulation of **Zone V**. In the northern part of the lake sediment input was high in particular in the vicinity of LP20 where 0.43 t m^{-2} accumulated in this period. All the cores from the southern part of the lake together with LP5 and LP6 display very low values of sediment input during this phase of disturbance being as low as 0.006 t m^{-2} .

The total amount of sediment input into the lake during this period of disturbance is estimated to be 13,339,224 tonnes which entered the lake at an average rate of $10,261 \text{ t yr}^{-1}$ and is equivalent to an erosion rate within the catchment of $12.8 \text{ t km}^{-2} \text{ yr}^{-1}$.

9.7.2 Zone IV (1,200-850 years B.P.)

Both the physical and chemical properties of the cores indicated that sediments associated with **Zone VI**, accumulated during a period of relative stability within the basin. These findings are supported by the results of this analysis which indicate a considerable reduction in sediment input over this period. Approximately 1,553,534 tonnes of sediment were deposited into the lake between 1,200 and 850 years B.P. at an average rate of $4,439 \text{ t yr}^{-1}$ (table 9.6). This represents an average soil loss of $5.8 \text{ t km}^{-2} \text{ yr}^{-1}$ from the drainage basin. Thus, sediment input during this period was about 35% of that during the preceding period of disturbance.

The most obvious difference is found in the Northern Basin where a considerable drop in sediment accumulation is noted. In Polygon One, for example, sediment input was at a rate of 269 t yr^{-1} compared to $1,730 \text{ t yr}^{-1}$ during the accumulation of **Zone V**. This represents a decrease in sediment input of 85% during

Polygon No.	Core No.	Thickness of layer (cm)	Mean Bulk Density	Mean CaCO ₃ Content %	Mean L.O.I %	Mean SiO ₂ %	Mean % Clastic Sediment	Polygon m ²	t/m ²	Total tonnes	t/yr
1	20	120	0.47	6	12	4	78	511422.0	0.43	2249838	1730
2	19	57	0.40	5	14	4	77	4761077	0.17	835841	642
3	18	85	0.33	5	13	4	78	5302155	0.22	1087977	892
4	17	55	0.38	5	14	4	77	4972778	0.16	1082801	833
5	16	52	0.30	9	15	4	72	6728463	0.11	596890	459
6	14	25	0.38	12	13	4	71	5314241	0.067	358442	276
7	15	100	0.35	10	12	7	71	4671128	0.25	1160768	893
8	13	73	0.35	1	12	7	80	2334812	0.20	477233	366
9	9	85	0.33	5	16	7	72	2789643	0.20	563387	434
10	10	85	0.32	2	13	7	78	5350787	0.21	1135204	876
11	8	60	0.27	9	11	7	76	3563847	0.12	438775	337
12	7	120	0.30	4	12	5	79	6062597	0.28	1724175	1326
13	MC	70	0.27*	4	12	5	79	5233226	0.15	781369	601
14	6	23	0.25	11	14	5	70	4594711	0.04	184936	142
15	5	22	0.31	14	15	5	66	8627296	0.045	388327	298
16	4	16	0.28	9	17	5	69	3268616	0.031	101038	78
17	12	8	0.19	34	20	5	41	2072629	0.006	12916	10
18	3	14	0.28	8	18	5	72	786115	0.028	22186	17
19	11	40	0.27	8	15	5	72	1185693	0.077	92192	71
20	1	8	0.23	21	13	5	41	1373773	0.008	10363	8
21	2	6	0.19	10	13	5	72	4211383	0.008	34566	27
Total input for lake =										13,339224t	10261 t/yr

Table 9.5 Variations in clastic input into Lake Pátzcuaro between 2,500 and 1,200 years ago.

Polygon No.	Core No.	Thickness of layer (cm)	Mean Bulk Density	Mean CaCO ₃ Content %	Mean L.O.I. %	Mean SiO ₂ %	% Clastic Sediment	Polygon m ²	t/m ²	tonnes	Total t/yr
1	20	12	0.24	19	13	4	64	511422.0	0.018	94265	269
2	19	20	0.23	27	17	4	52	4761077	0.023	113884	325
3	18	27	0.23	25	15	4	56	5302155	0.034	184387	526
4	17	20	0.20	14	11	4	71	4972778	0.028	141224	403
5	16	15	0.19	19	24	4	53	6728463	0.015	101632	290
6	14	13	0.23	27	19	4	50	5314241	0.015	79447	226
7	15	7	0.16	29	19	6	46	4671128	0.005	24005	68
8	13	13	0.16	19	21	6	54	2334812	0.011	26224	75
9	9	13	0.17	14	19	6	61	2789643	0.013	37606	107
10	10	18	0.21	13	21	6	60	5350787	0.027	121353	346
11	8	8	0.19	20	15	6	59	3563847	0.009	31960	91
12	7	12	0.21	13	22	6	59	6062597	0.015	90137	257
13	MC	15	0.20	30	20	6	44	5233226	0.013	69078	197
14	6	18	0.19	16	28	6	60	4594711	0.021	94283	269
15	5	10	0.20	5	22	6	67	8627296	0.013	115604	330
16	4	25	0.19	14	23	10	53	3268616	0.025	82287	235
17	12	10	0.20	29	22	10	39	2072629	0.008	16166	46
18	3	13	0.20	24	32	10	34	786115	0.008	6949	10
19	11	12	0.19	7	22	10	61	1185693	0.014	27031	77
20	1	8	0.16	7	21	10	62	1373773	0.008	10901	31
21	2	22	0.17	16	18	10	54	4211383	0.020	85051	243
Total input for lake =										1553534t	4439 t/yr

Table 9.6 Variations in clastic input into Lake Pátzcuaro between 1,200 and 850 years ago.